

AD \_\_\_\_\_

Award Number: W81XWH-11-1-0646

TITLE: Novel Therapeutic Targets for Chronic Migraine

PRINCIPAL INVESTIGATORS: Andrew Charles

CONTRACTING ORGANIZATION: University of California, Los Angeles  
Los Angeles CA 90095

REPORT DATE: September 2013

TYPE OF REPORT: Annual Report

PREPARED FOR: U.S. Army Medical Research and Material Command  
Fort Detrick, Maryland 21702-5012

DISTRIBUTION STATEMENT: Approved for Public Release;  
Distribution Unlimited

The views, opinions and/or findings contained in this report are those of the author(s) and should not be construed as an official Department of the Army position, policy or decision unless so designated by other documentation.

# REPORT DOCUMENTATION PAGE

*Form Approved  
OMB No. 0704-0188*

Public reporting burden for this collection of information is estimated to average 1 hour per response, including the time for reviewing instructions, searching existing data sources, gathering and maintaining the data needed, and completing and reviewing this collection of information. Send comments regarding this burden estimate or any other aspect of this collection of information, including suggestions for reducing this burden to Department of Defense, Washington Headquarters Services, Directorate for Information Operations and Reports (0704-0188), 1215 Jefferson Davis Highway, Suite 1204, Arlington, VA 22202-4302. Respondents should be aware that notwithstanding any other provision of law, no person shall be subject to any penalty for failing to comply with a collection of information if it does not display a currently valid OMB control number. PLEASE DO NOT RETURN YOUR FORM TO THE ABOVE ADDRESS.

<b>1. REPORT DATE</b> Septbember 2013			<b>2. REPORT TYPE</b> Annual Report		<b>3. DATES COVERED</b> 1 September 2012- 31 August 2013	
<b>4. TITLE AND SUBTITLE</b>  Novel Therapeutic Targets for Chronic Migraine			<b>5a. CONTRACT NUMBER</b>			
			<b>5b. GRANT NUMBER</b> W81XWH-11-1-0646			
			<b>5c. PROGRAM ELEMENT NUMBER</b>			
<b>6. AUTHOR(S)</b>  Andrew Charles  E-Mail: acharles@ucla.edu			<b>5d. PROJECT NUMBER</b> PR100085		<b>5e. TASK NUMBER</b>	
			<b>5f. WORK UNIT NUMBER</b>		<b>8. PERFORMING ORGANIZATION REPORT NUMBER</b>	
			<b>9. SPONSORING / MONITORING AGENCY NAME(S) AND ADDRESS(ES)</b> U.S. Army Medical Research and Materiel Command Fort Detrick, Maryland 21702-5012		<b>10. SPONSOR/MONITOR'S ACRONYM(S)</b>	
<b>12. DISTRIBUTION / AVAILABILITY STATEMENT</b> Approved for Public Release; Distribution Unlimited			<b>11. SPONSOR/MONITOR'S REPORT NUMBER(S)</b>			
<b>13. SUPPLEMENTARY NOTES</b>						
<b>14. ABSTRACT</b> Chronic migraine is a disabling disorder that affects millions of individuals worldwide, and may result from traumatic brain injury. The purpose of this study is to use rodent models of basic migraine mechanisms to characterize new potential treatments for chronic migraine. The scope of the research is to investigate multiple novel potential drug treatments on migraine-related brain excitability, pain-sensing mechanisms, and behavior. The major findings of the research in the second year of the project are that the medications memantine causes a small reduction in chronic migraine-related hyperalgesia in mice. Amiloride also prevents the development chronic migraine-related hyperalgesia in mice. These results support the clinical investigation of amiloride and related drugs as treatments for chronic migraine. We have also found that the drug memantine inhibits cortical spreading depression, but acute treatment with memantine does not inhibit nociceptive signaling in the brainstem. These results are consistent with the potential efficacy of memantine as a preventive therapy, but not as an acute therapy for migraine. We have also found that delta opioid receptor agonists inhibit both cortical spreading depression and migraine related pain behaviors, also supporting the clinical investigation of these compounds. Overall, we have made significant progress in the characterization of novel potential therapies for chronic migraine.						
<b>15. SUBJECT TERMS</b> Migraine, Therapy, Amiloride, Memantine, Canrenone						
<b>16. SECURITY CLASSIFICATION OF:</b>			<b>17. LIMITATION OF ABSTRACT</b>  UU	<b>18. NUMBER OF PAGES</b>  53	<b>19a. NAME OF RESPONSIBLE PERSON</b> USAMRMC	
<b>a. REPORT</b> U	<b>b. ABSTRACT</b> U	<b>c. THIS PAGE</b> U	<b>19b. TELEPHONE NUMBER</b> (include area code)			

## **Table of Contents**

	<u>Page</u>
<b>Introduction .....</b>	<b>4</b>
<b>Body.....</b>	<b>4-8</b>
<b>Key Research Accomplishments .....</b>	<b>8-9</b>
<b>Reportable Outcomes .....</b>	<b>9-10</b>
<b>Conclusion .....</b>	<b>10</b>
<b>References .....</b>	<b>NA</b>
<b>Appendices.....</b>	<b>10-...</b>

**INTRODUCTION:** This project investigates basic mechanisms of migraine, a disorder that afflicts hundreds of millions of individuals worldwide. Chronic migraine, defined as more than 15 days of headache per month, affects 4% of the population and is a particularly disabling condition. Traumatic brain injury is a common trigger for common migraine.

**BODY:**

The progress on each of the originally proposed tasks is summarized below.

**Task 1. Characterization of the effects of memantine on migraine models**

a. **Effects of memantine on CSD-** We are continuing to investigate the effects of memantine on the propensity to CSD and associated changes in neuovascular coupling.

b. **Effects of memantine on trigeminovascular nociceptive activation.** Studies by the Goadsby group indicate that despite the fact that the NR-1 glutamate receptor subunit is expressed and memantine inhibits glutamate-evoked signaling in the trigeminocervical complex, memantine *does not* inhibit trigeminovascular nociceptive activation in rats.

**1. Immunohistochemical characterization of NR1 receptor in the trigeminocervical complex**

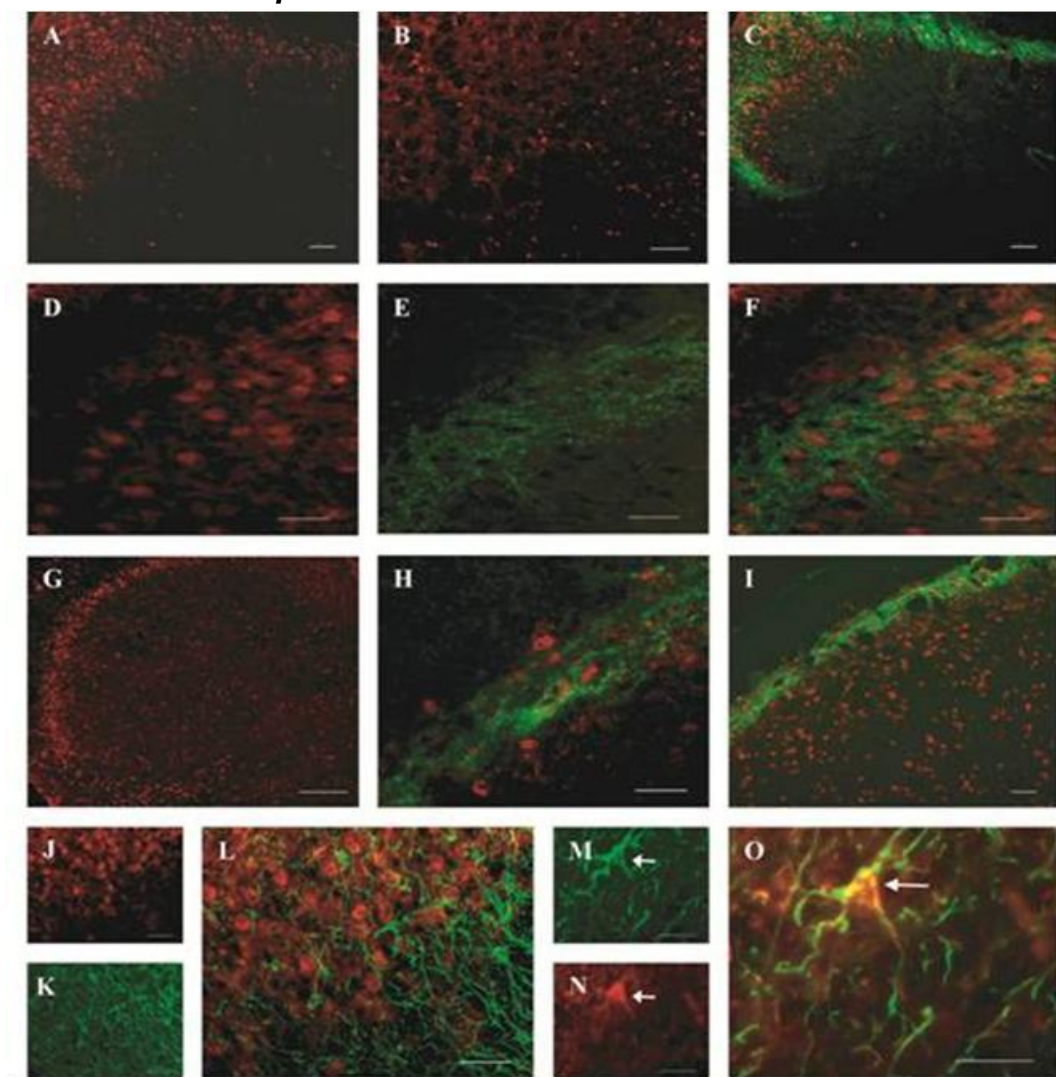


**Figure 1.** Representative distribution of NR1-like immunoreactivity (labeled with Texas red-avidin) in the dorsal region of the cervical spinal cord at C2 (A, B, C), C1 (D, E, F) and trigeminal nucleus caudalis (TNC; G, H, I) is shown. Photomicrographs (original magnification,  $\times 100$ ) show NR1-like immunoreactivity in C2 (A) and a higher magnification ( $\times 200$ ) shows scattered cells in deeper C2 laminae IV–V (B). NR1-like immunoreactive cells are localized near calcitonin gene-related peptide (CGRP)-like immunoreactive fibers in C2 (C; labeled with fluorescein isothiocyanate) original magnification  $\times 100$ ). High magnification photomicrographs (original magnification,  $\times 400$ ) show the intracellular aspect of NR1-like immunoreactivity in laminae I and II at the cervical spinal cord at C1 (D; note the punctuate appearance of the staining restricted to the cytoplasm in the soma), the CGRP-like staining in laminae I and outer lamina II, and their colocalization in these laminae (E). Photomicrographs (original magnification,  $\times 50$ ) show NR1-like immunoreactivity in the trigeminal nucleus caudalis (TNC; G) and its colocalization with CGRP in the superficial laminae of the TNC (H; original magnification,  $\times 400$ ). A representative TNC section (original magnification,  $\times 100$ ) stained for CGRP and NeuN-like immunoreactivity (the latter labeled with Texas red; I), suggests that not all neurons express the NR1 protein. (J–O) Double labeling of NR1- and GFAP-like immunoreactivity shows astrocytes in green (J–L; original magnification  $\times 100$ ; M–O; original magnification,  $\times 1000$ ; note the colocalization of NR1 and GFAP on panel L). Only few astrocytes express NR1-like immunoreactivity (M–O; white arrows). Scale bars = 50  $\mu\text{m}$  (D–F, H, J–O), 100  $\mu\text{m}$  (A–C, I), 500  $\mu\text{m}$  (G).

## **Figure 2. Effect of microiontophoretic application of memantine onto trigeminocervical neurons**

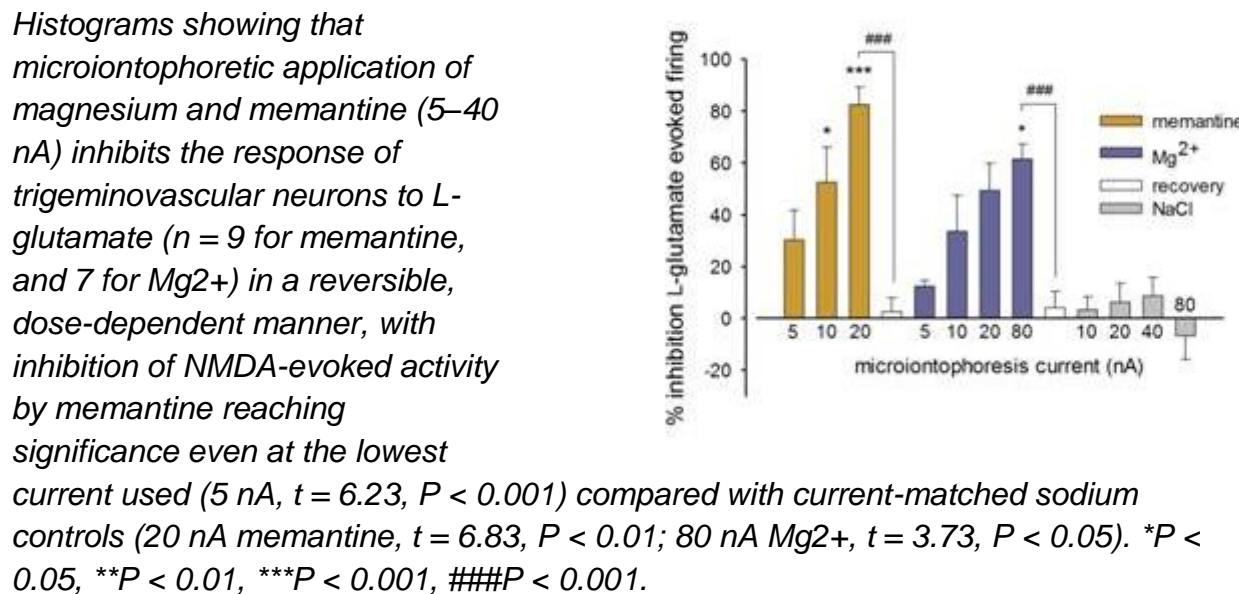
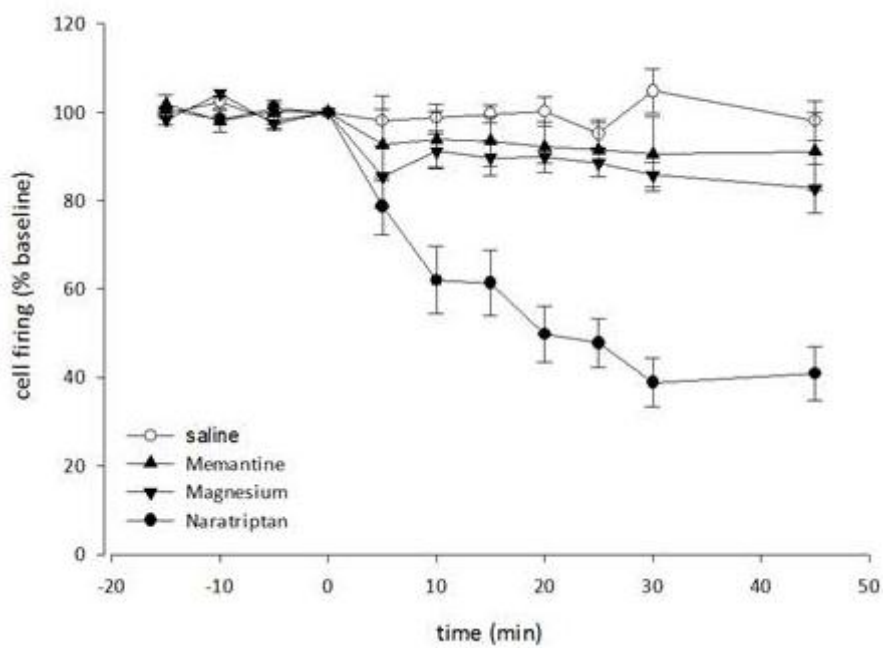


**Figure 3. Effects on electrically stimulated MMA-evoked firing of intravenous administration of memantine**

Cell firing in response to nociceptive trigeminovascular activation comparing the effects of magnesium (100 mg/kg), memantine (10 mg/kg), and naratriptan (5 mg/kg) demonstrates no effect of memantine or magnesium. For an active control naratriptan is demonstrated to be effective in this model.

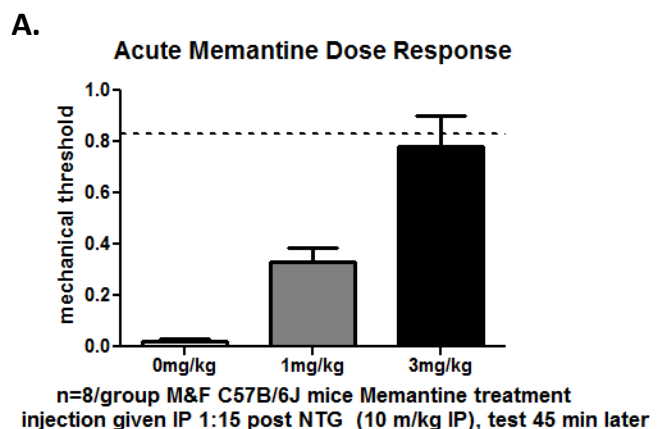


**c. Effects of memantine on acute and chronic nitroglycerin-evoked hyperalgesia in mice:**

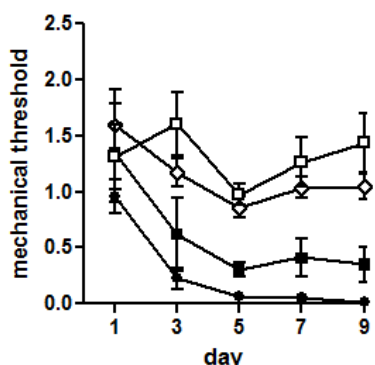
**Figure 4 Memantine inhibits acute but not chronic NTG-evoked hyperalgesia.**

A. Dose dependent increase in mechanical threshold in response to memantine

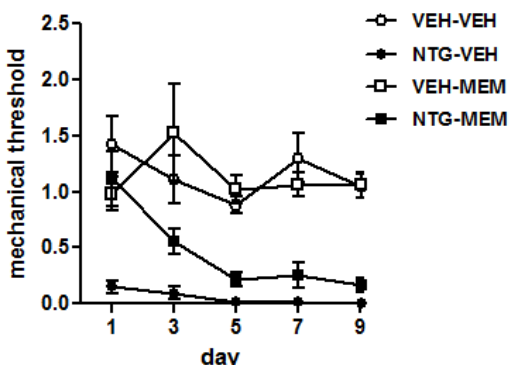
B. Memantine minimally inhibits chronic basal hyperalgesia and inhibits acute hyperalgesia only on days 1 and 3 of NTG administration



**B.** **Baseline**



**Post-Injection**



*Conclusions* - The results indicate that while memantine inhibits migraine-related cortical excitability, it does not inhibit chronic nitroglycerin-evoked hyperalgesia or trigeminovascular nociceptive activation. These mixed results do not provide strong support for the potential efficacy of memantine as a preventive therapy in chronic migraine or post-traumatic headache.

***Task 2. Characterization of the effects of amiloride on migraine models***

- a. *Effects of amiloride on cortical spreading depression*
  - b. *Effects of amiloride on trigeminovascular nociceptive activation*
  - c. *Effects of amiloride on acute and chronic nitroglycerin-evoked hyperalgesia in mice*
- These studies were performed in Year 1 of the project (See Appendix 1). Amiloride's effects on multiple migraine mechanisms supports formal clinical investigation as a preventive therapy for migraine and post-traumatic headache.

***Task 3. Characterization of the effects of canrenone on migraine models***

Work on these studies is beginning.

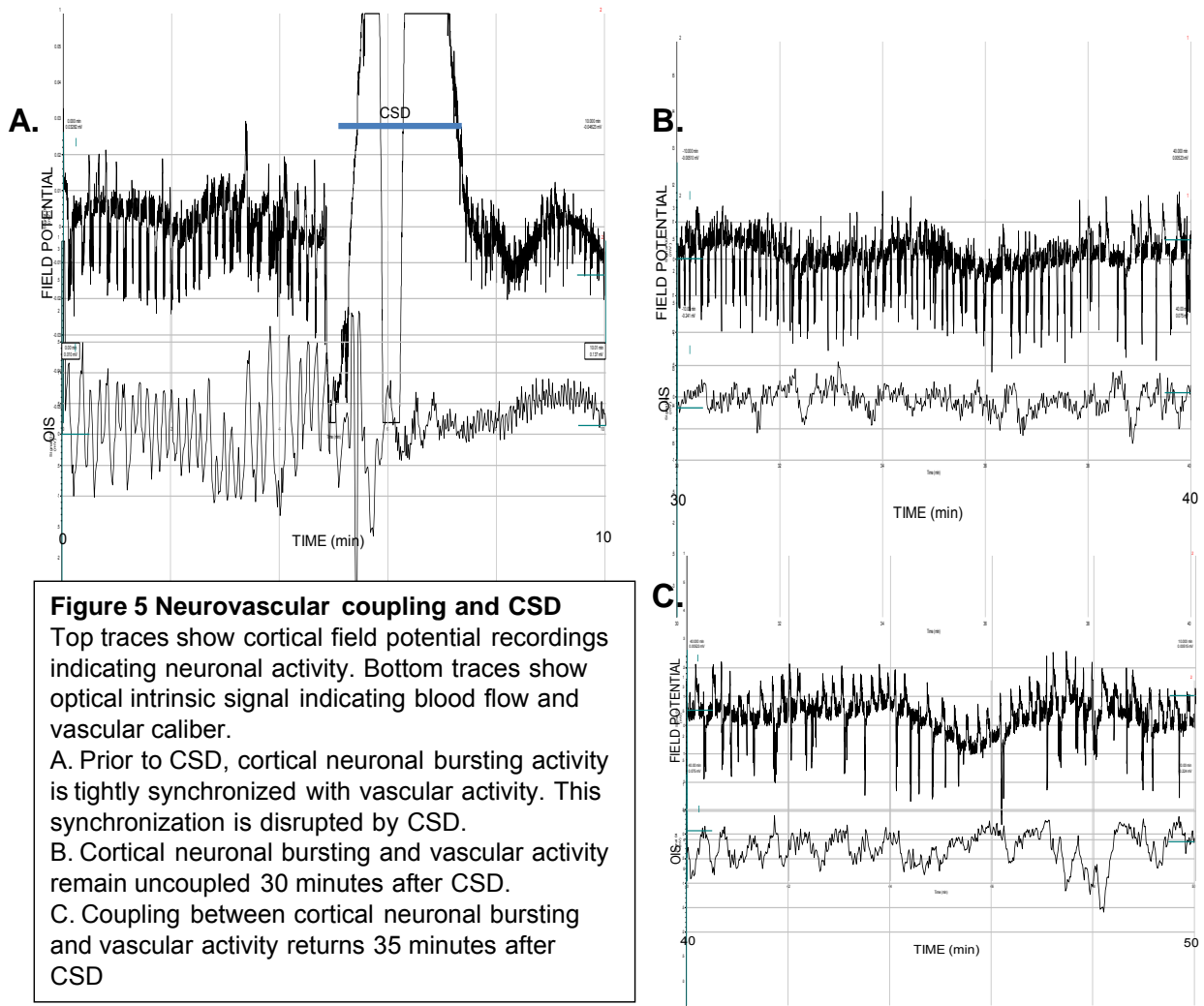
*Additional accomplishments*

***Effects of Migraine Preventive Therapies on Chronic Nitroglycerin-evoked Hyperalgesia***

We have refined the nitroglycerin (NTG) model of chronic migraine with a variety of studies including investigation of the effects of multiple medications (Appendix #2). We have shown that NTG-evoked hyperalgesia is potentiated by the phosphodiesterase inhibitor sildenafil, confirming a nitric oxide-mediated mechanism for the phenomenon. We have also performed studies of the established migraine preventive therapies topiramate and propranolol, on the chronic nitroglycerin evoked hyperalgesia model of chronic migraine. We have found that both of these medications inhibit chronic hyperalgesia, providing additional support for the translational validity of this model.

***Neurovascular uncoupling following CSD - a potential therapeutic target***

We have performed additional analysis of the physiological consequences of cortical spreading depression (CSD), characterizing in detail the disruption of the normal coupling between neuronal activity and vascular activity that occurs for 30-50 minutes following CSD. We believe that this neurovascular uncoupling represents a potentially important therapeutic target, and we have begun investigating the effects of acute and preventive migraine therapies on this target.



### Mutations in casein kinase 1 $\delta$ in migraine

We completed studies demonstrating that mutations in the gene encoding casein kinase 1 $\delta$  segregate with migraine in 2 families, and that mice expressing one of these mutations show multiple characteristics consistent with a migraine phenotype including increased hyperalgesia and a reduced threshold for cortical spreading depression. This project supported the effort of the PI in bringing these results to publication (Appendix 3).

### KEY RESEARCH ACCOMPLISHMENTS:

- Acute administration of memantine inhibits acute hyperalgesia, but chronic administration of memantine results in a modest reduction in chronic migraine-related hyperalgesia. Although the NR-1 subunit of the glutamate receptor is present and memantine inhibits glutamate mediated signaling in the trigeminocervical complex, memantine does not inhibit trigeminovascular nociceptive signaling. These studies do not support the clinical use of memantine as a therapy for migraine .
- Further validation of chronic nitroglycerin-evoked hyperalgesia as a translational model for the study of chronic migraine and preventive therapies.

- Identification of neurovascular uncoupling following cortical spreading depression as an additional therapeutic target.
- Mice expressing mutations in the gene encoding casein kinase 1 $\delta$  represent a novel model for migraine

## **REPORTABLE OUTCOMES:**

### *Manuscripts:*

Holland PR, Akerman S, Andreou AP, Karsan N, Wemmie JA, Goadsby PJ. Acid-sensing ion channel 1: a novel therapeutic target for migraine with aura. *Annals of Neurology* 2012;72(4):559-63.

Pradhan, A., Smith, M., McGuire, B., Tarash, I., Evans, C., and A.C. Charles. Characterization of a novel model of chronic migraine. *Pain*. Accepted pending minor revisions, 2013.

Brennan, K.C., E.A. Bates, R.E. Shapiro, J. Zyuzin, W.C. Hallows, Y. Huang, H.Y. Lee, C.R. Jones, Y.H. Fu, A.C. Charles\*, and L.J. Ptacek\*. (\*Co-corresponding authors) Casein kinase delta mutations in familial migraine and advanced sleep phase. *Science Translational Medicine*. 5:183ra156, 181-111, 2013.

Charles A. Migraine: a brain state. *Current opinion in neurology*. 26:235-9, 2013.

### *Abstracts/presentations:*

Hoffmann J, Park JW, Storer RJ, Goadsby PJ. Magnesium and memantine do not inhibit nociceptive neuronal activity in the trigeminocervical complex of the rat. Journal of Headache and Pain. 2013;1(Suppl 1):P71.

A.A. Pradhan, B. McGuire, A. Charles Characterization of a novel model of migraine European Headache and Migraine Trust International Conference London 2012.

A. Pradhan. The National Headache Foundation Lectureship Award (February 2012)The Potential of Delta Opioid Receptor Agonists for the Treatment of Migraine.

M.Smith, J. Zyuzin, A.Charles, and A. A. Pradhan. The delta opioid receptor as a novel therapeutic target for the treatment of migraine. Society for Neuroscience, New Orleans 2012.

A.A. Pradhan. A Screen of Prophylactic Anti-Migraine Medications in a Chronic Nitroglycerin Mouse Model. International Headache Conference Boston June 2013.

A. Charles - International Headache Congress Presidential Symposium. "Migraine Science: New Opportunities for Greater Understanding and Better Therapies".

**Funding applied for based on work supported by this award**

NIH RO1 - Andrew Charles and Peter Goadsby, Co-PI's, "Novel Migraine Mechanisms as Targets for Therapy"

**CONCLUSION:** In the second year of this project we have continued to make significant progress in the investigation of the effects of potential treatments on basic mechanisms of migraine. We have provided further evidence in support of the translational validity of chronic nitroglycerin-evoked hyperalgesia as a model for chronic migraine. Based on our pre-clinical models, the medication memantine does not show promise as a therapy for chronic migraine. We have enhanced our understanding of the physiological effects of cortical spreading depression (CSD), and we will now investigate the potential of migraine therapies to improve neurovascular coupling after CSD. We are in an excellent position to make further progress toward a better understanding of basic migraine mechanisms and to bring new therapies to patients with this disabling disorder.

**REFERENCES:** None

**APPENDICES:**

Holland PR, Akerman S, Andreou AP, Karsan N, Wemmie JA, Goadsby PJ. Acid-sensing ion channel 1: a novel therapeutic target for migraine with aura. **Annals of Neurology**. 2012;72(4):559-63.

Pradhan, A., Smith, M., McGuire, B., Tarash, I., Evans, C., and A.C. Charles. Characterization of a novel model of chronic migraine. **Pain**. Accepted pending minor revisions, 2013..

Brennan, K.C., E.A. Bates, R.E. Shapiro, J. Zyuzin, W.C. Hallows, Y. Huang, H.Y. Lee, C.R. Jones, Y.H. Fu, A.C. Charles\*, and L.J. Ptacek\*. (\*Co-corresponding authors) Casein kinase delta mutations in familial migraine and advanced sleep phase. **Science Translational Medicine**. 5:183ra156, 181-111, 2013.

Charles A. Migraine: a brain state. **Current opinion in neurology**. 26:235-9, 2013.

# Acid-Sensing Ion Channel 1: A Novel Therapeutic Target for Migraine with Aura

Philip R. Holland, PhD,<sup>1,2</sup> Simon Akerman, PhD,<sup>1</sup> Anna P. Andreou, PhD,<sup>1</sup>  
Nazia Karsan, MB, ChB,<sup>1</sup> John A. Wemmie, PhD,<sup>3</sup> and Peter J. Goadsby, MD, PhD<sup>1</sup>

**Objective:** Migraine with aura is a severe debilitating neurological disorder with few relatively specific therapeutic options.

**Methods:** We used amiloride, a blocker of epithelial sodium channels, to evaluate its pharmacological potential and explored the biology of a potential mechanism of action in well-established experimental models.

**Results:** Amiloride was shown to block cortical spreading depression, the experimental correlate of aura, and inhibited trigeminal activation in *in vivo* migraine models, via an acid-sensing ion channel 1 mechanism. Remarkably, amiloride then demonstrated good clinical efficacy in a small open-labeled pilot study of patients, reducing aura and headache symptoms in 4 of 7 patients with otherwise intractable aura.

**Interpretation:** The observations here identify an entirely novel treatment strategy for migraine.

ANN NEUROL 2012;72:559–563

Migraine is a common neurological disorder with an annual prevalence of at least 12%,<sup>1</sup> costing nearly \$20 billion in the United States alone.<sup>2</sup> Approximately 20 to 30% of patients report aura,<sup>3</sup> focal neurological disturbances thought to be an expression of the experimental phenomenon of cortical spreading depression (CSD).<sup>4</sup> The most urgent unmet clinical need in migraine therapeutics is the provision of new approaches to preventive treatment, with only about 1/3 of patients who might require it currently being treated.<sup>5</sup> Even with knowledge of several mutations in familial forms of migraine,<sup>6</sup> there is a dearth of novel compounds in phase II development.

Amiloride is known to block the widely expressed epithelial sodium channels (ENaCs)/degenerin gene family,<sup>7</sup> which includes the acid-sensing ion channels (ASICs). The ASICs represent proton-gated channels that are able to flux Na<sup>+</sup> and Ca<sup>2+</sup> and are encoded by 4 genes responsible for 6 different subunits. ASIC1, which is encoded by the *ACCN2*<sup>7</sup> gene, has been linked to a variety of functions ranging from mechanotransduction to seizure termination<sup>8</sup> and neuroprotection.<sup>9</sup> Pharmacological blockade or transgenic deletion of the ASICs has

been shown to protect against tissue damage in models of multiple sclerosis and ischemic brain injury.<sup>9</sup> Given the known involvement of ASICs in seizurelike behavior,<sup>8</sup> the induction of tissue hypoxia and disruption by CSD<sup>10</sup> and the further comorbidity data between migraine and epilepsy,<sup>11</sup> as well as that a number of anti-epileptic agents are proven preventive treatments in migraine,<sup>12</sup> we proposed that blockade of the amiloride-sensitive ENaCs could be a novel beneficial treatment option for migraine, particularly for patients with aura.<sup>13</sup>

## Materials and Methods

Male Sprague Dawley rats and male age-matched wild-type and ASIC 1 knockout (ASIC1<sup>-/-</sup>) mice on a congenic C57Bl6 background were anesthetized with sodium pentobarbitone and maintained with propofol or isoflurane, respectively. A femoral artery and both femoral veins were cannulated (femoral vein only in mice) for blood pressure monitoring and intravenous infusion. Animals were placed in a stereotaxic frame and physiological parameters were maintained as detailed in the Supplementary Methods.

Cortical steady potentials (direct current [DC]; rat and mouse) and cerebral blood flow (rat only) were recorded (Supplementary Fig 1A) in response to needle prick or K<sup>+</sup>

View this article online at [wileyonlinelibrary.com](http://wileyonlinelibrary.com). DOI: 10.1002/ana.23653

Received Dec 19, 2011, and in revised form Apr 16, 2012. Accepted for publication May 4, 2012.

Address correspondence to Dr Goadsby, Headache Group, Department of Neurology, University of California at San Francisco, 1701 Divisadero St, Suite 480, San Francisco, CA 94115. E-mail: peter.goadsby@ucsf.edu or philip.holland@ed.ac.uk

From the <sup>1</sup>Headache Group, Department of Neurology, University of California at San Francisco, San Francisco, CA; <sup>2</sup>Centre for Neuroregeneration, University of Edinburgh, Edinburgh, United Kingdom; and <sup>3</sup>Department of Psychiatry, University of Iowa/Veteran's Affairs Hospital, Iowa City, IA.

Additional supporting information can be found in the online version of this article.

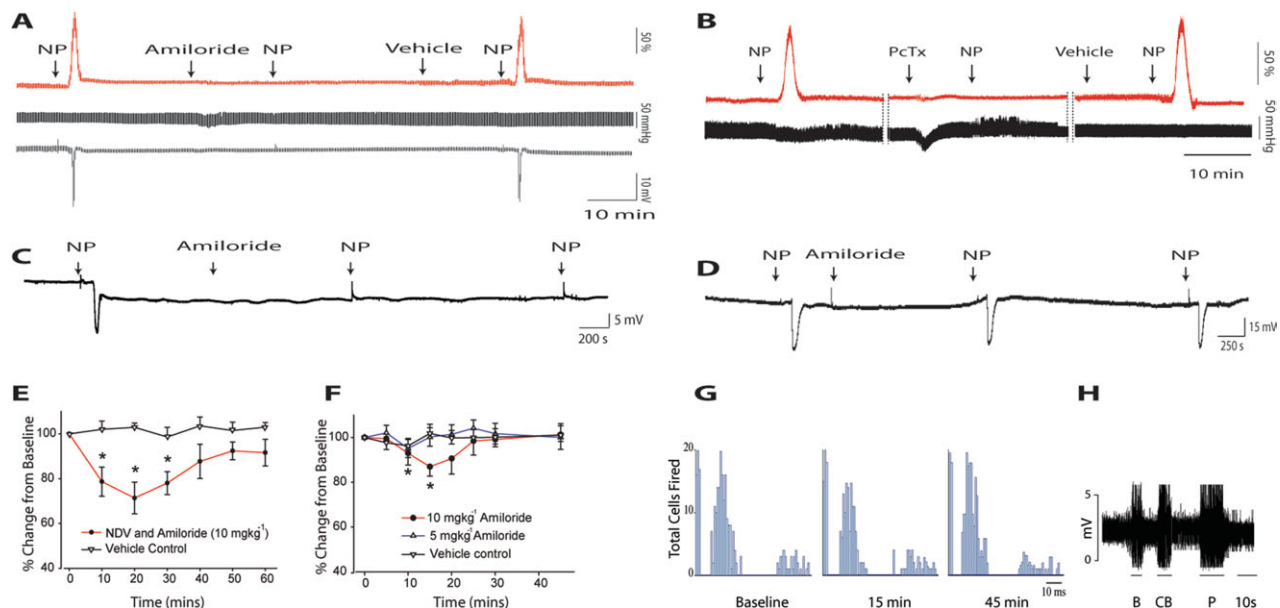


**FIGURE 1:** Acid sensing ion channel modulation in experimental models of migraine. (A) Regional cerebral blood flow (top), blood pressure (middle), and direct current shift (bottom) recordings from a sample cortical spreading depression (CSD) trace. Amiloride at 10mg/kg<sup>-1</sup> significantly inhibited needle prick (NP)-induced (6 of 8) CSDs when compared to vehicle controls ( $p = 0.007$ , Fisher exact test), despite having no significant effect on blood pressure. The lower dose of 5mg/kg<sup>-1</sup> had no significant effect on CSD propagation ( $p = 1.00$ , Fisher exact test), inhibiting only 1 of 8. (B) Regional cerebral blood flow (top) and blood pressure recordings from a sample CSD trace. Psalmotoxin (PcTx), the specific acid-sensing ion channel (ASIC) 1a blocker, significantly inhibited NP-induced CSDs (5 of 6) when compared to vehicle control ( $p = 0.015$ , Fisher exact test), but resulted in adverse blood pressure effects. (C, D) To characterize the likely action of amiloride, transgenic mice with targeted deletion of the ASIC1-producing ACCN2 gene were compared to age-matched wild-type controls. Amiloride significantly inhibited the number of CSDs propagating in the controls when compared to the ASIC1<sup>-/-</sup> mice ( $p = 0.049$ , Fisher exact test), with only 1 of 8 blocked in ASIC1<sup>-/-</sup> mice compared to 6 of 9 in controls. (E) Amiloride 10mg/kg<sup>-1</sup> inhibited neurogenic vasodilation (NVD;  $F_{6,42} = 5.1$ ,  $p < 0.001$ ;  $n = 8$ ) of the middle meningeal artery (MMA), maximally by 29% at 20 minutes postdrug ( $t_7 = 4.6$ ,  $p < 0.002$ ). (F) Effect of amiloride on trigeminal nucleus caudalis neuronal responses to stimulation of the dura mater surrounding the MMA. Amiloride at 10 but not 5mg/kg<sup>-1</sup> inhibited neuronal responses ( $F_{7,49} = 3.15$ ,  $p < 0.01$ ;  $n = 8$ ), significantly decreasing A-fiber responses at 10 and 15 minutes postdrug when compared to baseline and vehicle controls, maximally by 16%, returning to baseline levels after 20 minutes. (G) Original poststimulus histogram showing decreased A-fiber response 15 minutes post amiloride, returning to baseline levels after 45 minutes. (H) Original example of second-order trigeminal neuronal responses to facial receptive field stimulation, including light brush (B), corneal light brush (CB), and noxious pinch (P). Amiloride had no effect on any aspect of receptive field studied. [Color figure can be viewed in the online issue, which is available at [www.annalsofneurology.org](http://www.annalsofneurology.org).]

application to cortical surface to induce CSD following appropriate rest for refractory periods. Two control CSDs were always initiated to confirm reliable induction followed by a further 2 inductions with either amiloride (10 or 20mg/kg<sup>-1</sup>) or vehicle randomized to prevent ordering effects. For neurogenic dural vasodilation, a bipolar stimulating electrode was placed on the surface of the cranial window (see Supplementary Fig 1B), and vessel dilation was induced by stimulating at 5Hz for 10 seconds at increasing currents until maximal response was reached (100–200μA). After 2 baselines, amiloride (10mg/kg<sup>-1</sup>) was given as a bolus, and the effect on dilation was followed for 1 hour. Extracellular recordings were conducted in the trigeminal nucleus caudalis (TNC) in response to electrical square-wave stimuli (0.6Hz, 0.1–0.5-millisecond duration, 6–12V) applied onto the middle meningeal artery (MMA) to activate trigeminal afferents or cutaneous receptive field stimulation following amiloride (5 or 10mg/kg<sup>-1</sup>) or vehicle. Effects of drug intervention or gene deletion were analyzed using Fisher exact test due to the binary nature of CSD as an

all or nothing event (Prism version 5; GraphPad Software, La Jolla, CA), and total number of CSDs initiated as a result of K<sup>+</sup> induction following amiloride or vehicle control was compared using Student paired *t* test (SPSS version 12; SPSS Inc, Chicago, IL). The effects of stimulation on vessel diameter were calculated as a percentage increase from the prestimulation baseline. For electrophysiological recordings, the average of 3 baselines for comparisons was used or compared to vehicle control recordings. All intravital and electrophysiological data are expressed as mean ± standard error of the mean. Statistical analysis was performed using an analysis of variance for repeated measures with Bonferroni post hoc correction for multiple comparisons followed by Student paired *t* test (SPSS version 12.0) with significance at  $p < 0.05$ .

Five females and 2 males with medically refractory migraine with prolonged aura were offered amiloride. All patients had medically refractory migraine with persistent aura<sup>14</sup> and experienced discrete worsening of headache and aura symptoms. All patients had standard treatment trials of acetazolamide,

**TABLE: Patient Data on the Use of Amiloride**

Sex/Age, yr	Aura Phenotype	Length of History, yr	Medications in Addition to Standard Therapy <sup>a</sup>	Dose, mg/day	Outcome	Adverse Events
F/38	Visual, sensory, motor	7	Pizotifen, propranolol, verapamil	10	Nil effect	Mild reversible hyperkalemia
F/35	Visual, sensory, motor, brainstem	6	Pizotifen, propranolol, amitriptyline, verapamil	10	Aura symptoms settled by 75% and headache severity improved by 90%	Nil
F/47	Visual, sensory, motor	5	Pizotifen, propranolol, amitriptyline, methysergide	15	Nil effect	Polyuria
M/39	Visual, sensory, motor	6	Pizotifen, propranolol, amitriptyline, nifedipine	10	Aura symptoms and headache settled by 90%	Nil
F/45	Visual, sensory, motor	3	Pizotifen, propranolol, amitriptyline, nifedipine	10	Aura symptoms settled by 90% and headache severity improved by 80%	Nil
F/44	Visual, sensory, motor	8	Pizotifen, propranolol, amitriptyline	15	Aura symptoms settled by 70% and headache severity by 60%	Nil
M/47	Visual, sensory, motor, brainstem	7	Pizotifen, propranolol, amitriptyline, verapamil	20	Nil effect	Polyuria

<sup>a</sup>Standard treatment consisted of acetazolamide, flunarizine, lamotrigine, gabapentin, valproate, and topiramate to maximal doses, which were ineffective or not tolerated, or left significant attacks.

F = female; M = male.

flunarizine, lamotrigine, gabapentin, valproate, and topiramate to maximal doses, which were ineffective or not tolerated, or left significant attacks. All patients had had extensive investigation for underlying secondary causes, particularly prothrombotic states, including brain imaging, without a cause being identified. Patients were followed up from 6 to 24 months for responder outcome.

## Results

Cortical needle prick (NP)-induced CSD in rats produced a transient increase in cerebral blood flow in combination with a sharp deflection in DC potential (Fig 1). Administration of amiloride ( $10\text{mg/kg}^{-1}$ ) 15 minutes prior to NP significantly inhibited the number of NP-induced CSDs (6 of 8) when compared to vehicle, but failed to inhibit the number of  $\text{K}^+$ -induced CSDs (Supplementary

Results). To characterize the possible mechanism of action of amiloride, the effect of the specific ASIC1a blocker psalmotoxin (PcTx)<sup>15</sup> in the rat model of CSD was studied. PcTx (1:1,000;  $1.5\text{ml/kg}^{-1}$ ) demonstrated significant efficacy, blocking 5 of 6 NP-induced CSDs. We then explored a novel transgenic mouse that does not express ASIC1 due to deletion of the *ACCN2* gene.<sup>16</sup> Amiloride at  $10\text{mg/kg}^{-1}$  failed to block CSD in 3 control mice, and therefore the higher dose of  $20\text{mg/kg}^{-1}$  was used in mice. Administration of this higher dose significantly inhibited the propagation of NP-induced CSDs in wild-type mice (6 of 9) when compared to  $\text{ASIC1}^{-/-}$  mice, in which only 1 of 8 was blocked, suggesting that amiloride's anti-CSD actions are likely at least in part due to actions on the ASIC1 subunit and that ASIC1 may play a crucial role in CSD induction.

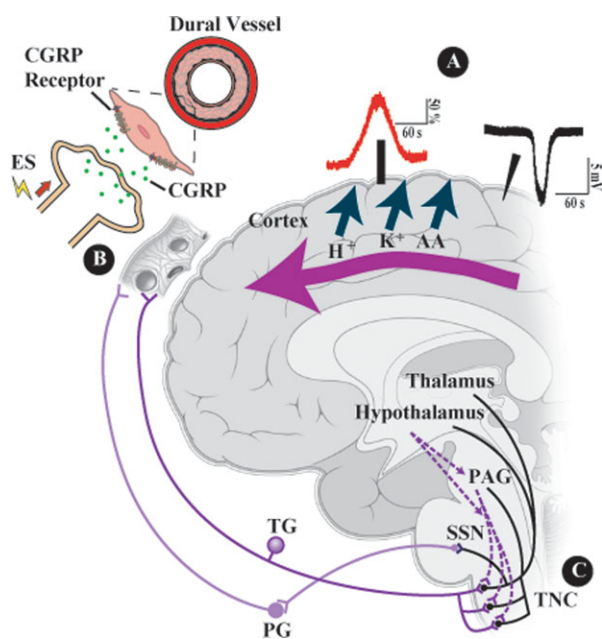


**FIGURE 2:** The proposed mechanisms of action of amiloride in the trigeminovascular system for the treatment of migraine with or without aura. The pseudounipolar trigeminal nerve conveys information from the dural vessels to the trigeminal nucleus caudalis (TNC) via the trigeminal ganglion (TG). Second-order neurons in the TNC then transmit this information to higher brain structures, including the contralateral thalamus and cortex. Modulatory pathways originating in the cortex, hypothalamus, and periaqueductal gray matter (PAG) among others send descending projections to the TNC, where they can modulate its activity. Amiloride demonstrates a diverse range of actions on the trigeminovascular system. It blocks needle prick-induced cortical spreading depression (CSD; purple arrow), which has been shown to increase c-fos in the TNC.<sup>19</sup> The exact mechanism of this activation is unclear, but may be due to direct primary afferent activation or interactions with descending inhibitory pathways (purple dashed lines), resulting in disinhibition.<sup>20</sup> (A) CSD results in a dramatic failure of brain ion homeostasis and the release of a variety of agents, including H<sup>+</sup>, K<sup>+</sup>, and arachidonic acid (AA). H<sup>+</sup> and AA are both known to potentiate acid-sensing ion channels,<sup>21</sup> which may aid the propagation of the spreading depression. In agreement, amiloride is efficacious in the treatment of aura and headache in migraine with aura patients. (B) Electrical stimulation (ES) of the cranial window over the middle meningeal artery (MMA) drives the release of calcitonin gene-related peptide (CGRP) from the prejunctional trigeminal nerve. CGRP activates CGRP receptors on the dural vessels, resulting in dural vasodilation, which is indicative of trigeminal nerve activation. Amiloride inhibits the observed neurogenic dural vasodilation, likely by inhibiting CGRP release, indicating a trigeminal primary afferent action. (C) Amiloride also inhibits TNC neuronal responses to MMA stimulation, demonstrating its ability to further modulate trigeminal nociceptive transmission. The intravenous route of administration may result in amiloride actions in other brain structures that are involved in the pathophysiology of migraine such as the thalamus, hypothalamus, and PAG. PG, pterygopalatine ganglion; SSN, superior salivatory nucleus.

We further studied amiloride's efficacy in 2 established models of trigeminal nociceptive processing in the rat. Electrical stimulation of the thinned cranium produced reproducible dilation of the MMA ( $118 \pm 12\%$ ;  $n = 8$ ) via trigeminally derived local calcitonin gene-related peptide (CGRP) release. This vasodilatation was significantly attenuated by  $10\text{mg/kg}^{-1}$  of amiloride, suggesting a direct action on the trigeminal nerve at the level of the dural vasculature (see Fig 1, 2). To test any central actions of amiloride, electrophysiological recordings were measured from 12 populations of neurons in the TNC, all of which were responsive to dural MMA stimulation and had receptive fields within the trigeminal facial dermatome (Supplementary Fig 2). Amiloride at  $10$  but not  $5\text{mg/kg}^{-1}$  significantly inhibited neuronal responses with A-fiber input to dural electrical stimulation when compared to vehicle, but had no effect on spontaneous neuronal firing or receptive field properties, suggesting no tonic action.

The efficacy of amiloride in blocking various animal models of migraine (Fig 2), especially NP-induced CSD, the relative lack of known adverse side effects, and open-label effects of other diuretics suggested its exploratory use in patients suffering from persistent aura who were particularly disabled, and had otherwise medically intractable symptoms. Remarkably, in this difficult to treat group of patients in whom standard treatment options had failed to provide sufficient symptomatic control, and whose outcome we audited for this report, amiloride substantially reduced both frequency of aura and headache severity in 4 of 7 patients receiving  $10$  to  $20\text{mg/day}^{-1}$ , followed up for between 6 and 24 months (Table).

## Discussion

Taken together, the data offer a strong indication that the ASIC1 subunit may offer a therapeutic target in migraine with aura, if not migraine more generally. The data support the development of specific compounds to target this receptor and the conducting of randomized placebo-controlled trials. Interestingly, amiloride was able to block NP-induced CSDs and showed further efficacy in 2 diverse models of trigeminovascular activation, suggesting multiple relevant sites of action. In agreement, amiloride reduced both the frequency of aura and the severity of pain in migraine with aura patients, suggesting a possible beneficial effect in migraine without aura. The failure of amiloride to inhibit K<sup>+</sup>-induced CSDs despite its efficacy in treating migraine aura suggests an interesting differentiation between the 2 experimental CSD-induction models, as previously highlighted.<sup>17</sup> Recent

data have indicated 2 distinct mechanisms for stimulating CGRP release from trigeminal ganglia neurons, either via a triptan responsive  $\text{Ca}^{2+}$ -dependent mechanism, or a likely  $\text{Na}^+$ -dependent proton-mediated activation of ASICs that is triptan nonresponsive.<sup>18</sup> Although the exact mechanisms involved need to be dissected, the clear efficacy of amiloride in experimental models and the indication of a clinical effect in migraine with aura patients suggest that ASICs are an option for a major therapeutic advance in a common and highly disabling neurological disorder.

## Authorship

P.R.H. and S.A. contributed equally to this study.

## Funding

This work was supported by the Sandler Foundation and the Department of Defense (PR100085P1).

## Potential Conflicts of Interest

P.R.H.: speaking fees, Almirall, Headache Cooperative of the Pacific. S.A.: consultancy, MSD, MAP Pharma/Allergan; employment, Eli Lilly; speaking fees, MSD; travel expenses, International Headache Society, American Headache Society. P.J.G.: board membership, Allergan, Colucid, MAP, Merck Sharpe & Dohme, eNeura, Neuromax, Autonomic Technologies, Boston Scientific, Eli Lilly, Medtronic, Linde, Bristol-Myers Squibb; consultancy, Pfizer, UCSF; grants/grants pending, GlaxoSmithKline, MAP, MSD, eNeura, Amgen; speaking fees, MSD, Pfizer, Allergan, Mennarini; paid educational presentations, American Headache Society.

## References

- Lipton RB, Diamond S, Reed M, et al. Migraine diagnosis and treatment: results from the American Migraine Study II. *Headache* 2001;41:638–645.
- Stewart WF, Ricci JA, Chee E, et al. Lost productive time and cost due to common pain conditions in the US workforce. *JAMA* 2003;290:2443–2454.
- Russell MB, Rasmussen BK, Fenger K, Olesen J. Migraine without aura and migraine with aura are distinct clinical entities: a study of four hundred and eight-four male and female migraineurs from the general population. *Cephalgia* 1996;16:239–245.
- Lauritzen M. Pathophysiology of the migraine aura. The spreading depression theory. *Brain* 1994;117:199–210.
- Lipton RB, Bigal ME, Diamond M, et al. Migraine prevalence, disease burden, and the need for preventive therapy. *Neurology* 2007;68:343–349.
- van den Maagdenberg AMJM, Haan J, Terwindt GM, Ferrari MD. Migraine: gene mutations and functional consequences. *Curr Opin Neurol* 2007;20:299–305.
- Kellenberger S, Schild L. Epithelial sodium channel/degenerin family of ion channels: a variety of functions for a shared structure. *Physiol Rev* 2002;82:735–767.
- Ziemann AE, Schnizler MK, Albert GW, et al. Seizure termination by acidosis depends on ASIC1a. *Nat Neurosci* 2008;11:816–822.
- Fries MA, Craner MJ, Etzensperger R, et al. Acid-sensing ion channel-1 contributes to axonal degeneration in autoimmune inflammation of the central nervous system. *Nat Med* 2007;13:1483–1489.
- Takano T, Tian GF, Peng W, et al. Cortical spreading depression causes and coincides with tissue hypoxia. *Nat Neurosci* 2007;10:754–762.
- Ottman R, Lipton RB. Is the comorbidity of epilepsy and migraine due to a shared genetic susceptibility? *Neurology* 1996;47:918–924.
- Goadsby PJ, Lipton RB, Ferrari MD. Migraine—current understanding and treatment. *N Engl J Med* 2002;346:257–270.
- Holland PR, Akerman S, Goadsby PJ. Amiloride-sensitive epithelial sodium channels: a novel therapy for migraine with aura? *Cephalgia* 2009;29:48.
- Headache Classification Committee of the International Headache Society. The International Classification of Headache Disorders (second edition). *Cephalgia* 2004;24:1–160.
- Escoubas P, De Weille JR, Lecoq A, et al. Isolation of a tarantula toxin specific for a class of proton-gated  $\text{Na}^+$  channels. *J Biol Chem* 2000;275:25116–25121.
- Wemmie JA, Chen J, Askwith CC, et al. The acid-activated ion channel ASIC contributes to synaptic plasticity, learning, and memory. *Neuron* 2002;34:463–477.
- Akerman S, Holland PR, Goadsby PJ. Mechanically-induced cortical spreading depression associated regional cerebral blood flow changes are blocked by  $\text{Na}^+$  ion channel blockade. *Brain Res* 2008;1229:27–36.
- Durham PL, Masterson C. Proton stimulation of CGRP secretion from trigeminal ganglia neurons occurs via an amiloride sensitive, calcium-independent mechanism and is not blocked by rizatriptan or botulinum neurotoxin type A. *Proc Soc Neurosci* 2010;54:G38.
- Bolay H, Reuter U, Dunn AK, et al. Intrinsic brain activity triggers trigeminal meningeal afferents in a migraine model. *Nat Med* 2002;8:136–142.
- Lambert GA, Truong L, Zagami AS. Effect of cortical spreading depression on basal and evoked traffic in the trigeminovascular sensory system. *Cephalgia* 2011;31:1439–1451.
- Wemmie JA, Price MP, Welsh MJ. Acid-sensing ion channels: advances, questions and therapeutic opportunities. *Trends Neurosci* 2006;29:578–586.

## **Characterization of a Novel Model of Chronic Migraine.**

**Abbreviated Title:** Model of chronic migraine

Amynah A Pradhan<sup>1,3,\$</sup>, Monique L Smith<sup>1,2,3</sup> Brenna McGuire<sup>2,3</sup>, Igal Tarash<sup>2,3</sup>, Christopher Evans<sup>1,3</sup>, and Andrew Charles<sup>2,3</sup>

<sup>1</sup>Semel Institute for Neuropsychiatry & Human Behavior, University of California Los Angeles

<sup>2</sup>Headache Research and Treatment Program, Department of Neurology David Geffen School of Medicine, UCLA

<sup>3</sup>Shirley and Stefan Hatos Center for Neuropharmacology, UCLA

\$To whom correspondence should be sent:

Dr. Amynah Pradhan

Semel Institute for Neuropsychiatry & Human Behavior

Hatos Center for Neuropharmacology

University of California Los Angeles

760 Westwood Plaza, Box 77

Los Angeles, CA 90024-1759

Tel 310-206-7883

Fax 310-825-7067

e.mail [amynahpradhan@ucla.edu](mailto:amynahpradhan@ucla.edu)

**# of Pages: 27**

**# Figures: 6**

**Conflict of Interest :** The authors declare no conflicts of interest.

**Acknowledgments :** This research was supported by the Department of Defense PR100085,

The Migraine Research Foundation, NIH-NIDA Grant DA05010, and the Shirley and Stefan

Hatos Research Foundation. AAP was supported by NIH-NIDA grant DA031243.

## ABSTRACT (250 words)

Chronic migraine is a disabling condition that affects millions of individuals worldwide. The development of novel migraine treatments has been slow, in part due to a lack of predictive animal models. We have developed a new model of chronic migraine involving the use of nitroglycerin, a known migraine trigger in humans. Chronic intermittent administration of nitroglycerin to mice resulted in acute mechanical hyperalgesia with each exposure as well as a progressive and sustained basal hyperalgesia. This chronic basal hyperalgesia occurred in a dose-dependent fashion and persisted for days following cessation of NTG administration. NTG-evoked hyperalgesia was exacerbated by the phosphodiesterase 5 inhibitor sildenafil, also a human migraine trigger, consistent with nitric oxide as a primary mediator of this hyperalgesia. The acute but not the chronic basal hyperalgesia was significantly reduced by the acute migraine therapy sumatriptan, whereas the chronic hyperalgesia was significantly reduced by the migraine preventive therapy topiramate. Chronic NTG-evoked hyperalgesia is a mouse model that may be useful for the study of mechanisms underlying progression of migraine from an episodic to a chronic disorder, and for the identification and characterization of novel acute and preventive migraine therapies.

## INTRODUCTION (500 words)

Migraine is one of the most common disorders affecting the general population, resulting in a staggering amount of episodic disability and lost productivity worldwide. For a significant percentage of patients it results in chronic disability [1-4]. Despite the extraordinarily high prevalence of migraine, our understanding of its pathophysiology is incomplete. Moreover, while there has been significant progress in the acute treatment of migraine attacks, the ability to treat frequent and chronically disabling migraine, remains severely limited. There continue to be millions of individuals for whom currently available migraine therapies are either ineffective or poorly tolerated [1; 2].

A significant obstacle to the identification of new migraine therapies has been the lack of predictive animal models. It has been particularly difficult to study the progression of migraine from an episodic to a chronic disorder. One approach to modeling acute migraine is the quantification of increased sensory sensitivity in response to known migraine triggers. Nitroglycerin (NTG) reliably triggers headache in normal subjects, and migraine without aura in migraine susceptible patients [5-8]; NTG-evoked migraine is a commonly used experimental paradigm in humans. (for review see [8; 9]). Nitroglycerin-evoked hyperalgesia in rodents has been developed as a model for sensory hypersensitivity associated with migraine [10; 11]. Acute nitroglycerin was previously shown to produce thermal and mechanical allodynia in mice that was reversed by the anti-migraine therapy sumatriptan [10]. In addition, in a transgenic mouse model of familial migraine, animals expressing a human migraine gene showed an even greater sensitivity to NTG-evoked hyperalgesia [12]. Further, NTG has also been shown to produce light-aversive behavior [11], and increased meningeal blood flow in mice [11; 13]. Taken together, these results indicate that the effects of NTG may effectively model migraine-like symptoms in rodents. Here we have extended the NTG-evoked hypersensitivity assays to model the progression of migraine from an acute to a chronic state.

## METHODS AND MATERIALS

### *Animals*

Subjects were male and female C57BL6/J mice, weighing 20–30g. Animals were housed in a 12-h light–dark cycle, and food was available *ad libitum*. All experiments were approved by the University Of California Los Angeles Office Of Animal Research, in accordance with AALAC guidelines. These experiments adhered to the guidelines of the Committee for Research and Ethical Issues of IASP [14].

### *Drug administration*

Nitroglycerin (NTG) was prepared from a stock solution of 5.0 mg/ml nitroglycerin in 30% alcohol, 30% propylene glycol, and water (American Regent). NTG was freshly diluted in 0.9% saline to a dose of 10 mg/kg. The vehicle control used in these experiments was 0.9% saline. We found that there was no significant difference in mechanical thresholds between those observed when 0.9% saline was used vs. those observed with 6% propylene glycol, 6% alcohol, 0.9% saline. All injections were administered as a 10 ml/kg volume. Unless otherwise noted, animals were tested for baseline responses immediately prior to intraperitoneal injection with nitroglycerin (NTG). Animals were injected with subsequent drugs (ip unless otherwise noted), 1h 15 min following NTG injection, and were tested for mechanical or thermal sensitivity 45 min later (2h post NTG). For chronic experiments, testing occurred every second day over 9 days (5 test days total). For the topiramate experiment, mice were injected with topiramate or vehicle every day for 11 days. On days 3,5,7,9, and 11 of this treatment, basal mechanical sensitivity was determined and mice received an injection of NTG or vehicle 1h15min prior to injection of topiramate/vehicle, and post-drug responses were determined 45 min later. For experiments testing localized intrathecal ijections of sumatriptan into the central nervous system, drug (0.06

$\mu$ g) or 0.9% saline was injected in a final volume of 5.0  $\mu$ l [15]. Intrathecal injections were performed with a 30 gauge, 1/2-inch needle at the L4-5 lumbar interspace on lightly restrained, unanesthetized mice.

#### *CFA-induced Inflammatory Pain*

Inflammatory pain was induced by injecting Complete Freund's Adjuvant (CFA, 1 mg *Mycobacterium tuberculosis* (H37Ra, ATCC 25177)/ml of emulsion in 85% paraffin oil and 15% mannide monooleate - Sigma) into the paw. Prior to the injection of CFA baseline mechanical responses (dashed line) were determined. Inflammation was induced by injecting 15  $\mu$ l of CFA into the plantar surface of the paw, and animals were subsequently tested 72h later.

#### *Sensory Sensitivity Testing*

To determine mechanical sensitivity, the threshold for responses to punctate mechanical stimuli (mechanical hyperalgesia) was tested according to the up-and-down method [16]. In brief, the plantar surface of the animal hindpaw was stimulated with a series of eight von Frey filaments (bending force ranging from 0.01 to 2 g). A response was defined as a lifting or shaking of the paw upon stimulation. The first filament tested was 0.4g. In the absence of a response a heavier filament (up) was tried, and in the presence of a response a lighter filament (down) was tested. This pattern was followed for a maximum of 4 filaments following the first response.

#### *Statistical Analysis*

Data are expressed as mean  $\pm$  s.e.m. All statistical analyses were performed by Sigmastat software. For all acute pain experiments, one-way ANOVAs were performed, and for chronic pain experiments a two-way repeated measures ANOVA was performed. Unless otherwise noted, all experiments were further analyzed using Holm-Sidak post-hoc analysis.

## RESULTS

### *Repeated administration of systemic nitroglycerin produces acute and chronic hyperalgesia*

Acute administration of nitroglycerin (NTG) has been shown previously to evoke severe mechanical and thermal hyperalgesia [10]. To model the progression to chronic migraine, we administered varying doses of NTG every second day for 9 days, resulting in a total of 5 NTG injections/test days. Mechanical thresholds were tested before and 2 hours after NTG administration on each test day. Nitroglycerin evoked significant acute mechanical hyperalgesia in a dose-dependent manner on each test day (Figure 1A). In addition, repetitive intermittent NTG administration over 9 days produced a significant time and dose-dependent chronic basal mechanical hyperalgesia as assessed by testing prior to each administration of NTG (Figure 1B). The greatest decrease in basal responses were observed with 10 mg/kg, the dose of NTG previously characterized in an acute study [10]. We chose to further characterize this dose (Figure 2). Significant acute hyperalgesia was again observed with each administration, and progressively increasing basal hyperalgesia was observed with repeated administration (Figure 2B, TREATMENT). Following the final treatment day (day 9), mechanical responses in mice were assessed daily to determine the recovery time for this basal hypersensitivity. Sensory responses returned to the level of naïve mechanical thresholds (day 1) by day 7 post-NTG (Figure 2B, day 16, RECOVERY). Female mice showed greater basal hyperalgesia in response to chronic NTG, and unlike males, basal sensitization was observed after a single NTG injection (Figure 2C, Day 3 NTG). To determine if the associative learning of repeated testing contributed to the progression of basal hyperalgesia, we examined basal mechanical thresholds in mice that had received identical intermittent NTG treatment over 9 days, but were only tested on the first day and the 9th day (novice). These novice mice did not show significantly different hyperalgesia on the final day of NTG (novice,  $0.15 \pm 0.06$  vs. repeatedly tested,  $0.05 \pm 0.03$ ).

*The Phosphodiesterase 5 inhibitor sildenafil increases acute and chronic mechanical hyperalgesia.*

To investigate the role of cGMP in NTG-induced basal and evoked hyperalgesia we examined the effects of the phosphodiesterase 5 inhibitor sildenafil, which increases levels of cGMP and augments the effects of nitric oxide (NO) as an activator of guanylate cyclase. We treated mice every second day for 9 days (5 test days) with a low dose of NTG (1 mg/kg ip), and sildenafil (3 mg/kg ip, Figure 3). On each day of testing, the combination of these two compounds produced a significantly greater acute hyperalgesia (Figure 3A), than either compound alone. In addition, while chronic treatment with this dose of NTG alone did not result in chronic basal hyperalgesia (Figure 3B), the combination of this low dose NTG with sildenafil produced significant basal hypersensitivity. Interestingly, by the final day of testing, sildenafil alone had also produced a significant decrease in basal mechanical threshold (Figure 3B). These results indicate changes in cGMP levels play a role in the hyperalgesia induced by chronic intermittent NTG treatment.

*Sumatriptan alleviates acute NTG-evoked, but not chronic basal hyperalgesia.*

We also investigated the effects of the migraine-selective acute therapy sumatriptan in the chronic NTG model. Consistent with previous studies [10], we found that sumatriptan (600 µg/kg, IP) reversed the acute hyperalgesia evoked by NTG injection. Sumatriptan continued to effectively ameliorate acute NTG-evoked hyperalgesia with each injection over 9 days. It did not, however, alter the chronic basal hyperalgesia that occurred over time with chronic intermittent NTG exposure (Figure 4A and B). These results indicate that while sumatriptan can reverse the acute effects of NTG, it does not reduce the progression of hyperalgesia that occurs with repeated exposure. To address the possibility that sumatriptan non-specifically inhibited nociception, we tested this same dose of sumatriptan within the Complete Freunds' Adjuvant (CFA) model of inflammatory pain. Sumatriptan (600 µg/kg ip) was ineffective at reversing CFA-

induced mechanical hyperalgesia (Figure 4C). To investigate the possibility that sumatriptan was acting to inhibit NTG-evoked mechanical hyperalgesia at the spinal level, we injected sumatriptan 0.06 µg (a dose previously shown to have anti-hyperalgesic effects in certain peripheral and visceral pain models [15]) or vehicle intrathecally into the spinal L4-5 region. In contrast to systemic intraperitoneal administration, intrathecal injection of sumatriptan did not result in any inhibition of NTG-evoked hyperalgesia (Figure 4D).

*Topiramate inhibited NTG-induced chronic basal hyperalgesia*

We then examined the effect of topiramate, a migraine preventive therapy, on acute and chronic basal hyperalgesia evoked by NTG. Mice were treated once daily with topiramate (30 mg/kg, IP) for 11 days. On days 3, 5, 7, 9, and 11 basal and acute NTG-evoked mechanical responses were determined. Daily treatment with topiramate significantly reduced acute NTG-evoked hyperalgesia and inhibited the development of chronic basal hyperalgesia induced by chronic intermittent NTG treatment (Figure 5A).

## DISCUSSION (1500 words)

Our results indicate that chronic intermittent treatment with nitroglycerin produces an acute and chronic hypersensitivity which could be a translationally significant model of chronic migraine. Repeated injection of NTG evoked mechanical hyperalgesia, which was blocked by the anti-migraine medication sumatriptan. We also found that chronic intermittent treatment with NTG produced a severe and long-lasting basal hyperalgesia, which was more pronounced in female mice. In addition, this basal hypersensitivity was alleviated by treatment with the migraine prophylactic, topiramate. Furthermore, the effects of concomitant treatment with another human migraine trigger, sildenafil, confirmed that this basal hypersensitivity was mediated by an increased levels of cGMP.

Several lines of evidence indicate that nitroglycerin treatment in rodents could be a predictive model of migraine in humans. Nitroglycerin is a reliable trigger of migraine in susceptible patients [5; 6; 8]. Interestingly, migraine attacks do not occur immediately after NTG administration with the vasodilatory effects of the drug, but rather after 2-6 hours [5; 6; 8], consistent with a delayed response to nitric oxide not mediated by vasodilation [17]. In mice, the timing of NTG-induced hyperalgesia also shows a delayed response, similar to the time course of headache observed in humans [10]. Systemic administration of NTG has been reported to cause cellular activation in nociceptive pathways, including trigeminal nociceptive pathways (REF), providing additional support for relevance to migraine. In addition, NTG has been shown previously to cause light allodynia [11], and to increase meningeal blood flow [11; 13] in mice, two hallmarks of migraine. Further, the amelioration of NTG-evoked hyperalgesia by they prototypic anti-migraine medication sumatriptan also supports this as a model for mechanisms of migraine. Finally, acute NTG-induced hyperalgesia has recently been shown to be increased in mice expressing a gene associated with familial migraine [12].

Migraine typically starts as an episodic disorder, but commonly progresses to a frequent or even daily condition [2]. The pathophysiological mechanisms underlying this change are poorly understood. We have extended the previously reported studies on acute NTG-evoked hyperalgesia to show that repetitive intermittent administration of NTG produces a progressive and sustained basal hyperalgesia that persists for days after the last exposure. These results are consistent with clinical observations of patients with chronic migraine in whom allodynia may occur both between and during migraine attacks. In addition, women are far more likely to suffer from chronic migraine than men, and the earlier development of basal hyperalgesia in female vs. male mice further validates this model. Previous studies have also shown that there are estrogen-related discrepancies in the brain regions activated with NTG administration in rats [18], again suggesting that the chronic NTG model could also be used as a tool to specifically study sex differences in migraine.

The enhancement of the effects of NTG by sildenafil, also an established human migraine trigger [9], provides evidence that NO-mediated increases in cGMP play a primary role in the hyperalgesia evoked by NTG. We found that by the final test day, sildenafil also independently produced basal hyperalgesia with repeated intermittent dosing, suggesting that potentiation of the endogenous activity of guanylate cylase may be a mechanism for producing chronic hyperalgesia. Drugs that target different aspects of the nitric oxide-cGMP pathway are currently being developed for the treatment of headache [9], and our preclinical data further support the role of this signaling cascade in the development of chronic migraine.

We found that sumatriptan inhibits acute hyperalgesia in response to NTG, similar to the results of previous studies <sup>11</sup>. We also found that sumatriptan continued to have this effect with each NTG exposure over time, but that it did not inhibit the resulting progressive chronic basal hyperalgesia. This result is consistent with the observation that while sumatriptan can be consistently effective as an acute migraine therapy, its use does not prevent progression of migraine over time [19]. Since this model tests hyperalgesia in the hindpaw, it is possible that

the effects of sumatriptan could be mediated by spinal mechanisms. However, we found that intrathecal administration of sumatriptan did not inhibit NTG-evoked mechanical hyperalgesia, in contrast to systemically administered sumatriptan; indicating that within this model sumatriptan is not acting primarily within the lumbar spinal cord. In addition, groups studying the dural inflammation model of migraine have also found that inflammatory mediators applied to the dura [20] or dural TRPA1 activation [21] produced mechanical hyperalgesia in both facial and hindpaw regions. Cutaneous allodynia following NTG likely reflects the development of central sensitization which is observed during primary headache, which may be mediated through sensitization of neurons within the thalamus [22].

Topiramate inhibited acute NTG-evoked hyperalgesia, as well as chronic basal hyperalgesia, consistent with its actions as a prophylactic migraine therapy. Topiramate has multiple mechanisms of actions that could be involved in its therapeutic efficacy for migraine, including inhibition of voltage gated sodium channels, enhancement of GABAergic signaling, inhibition of glutamatergic signaling, and inhibition of carbonic anhydrase [23]. It has been proven to be an effective preventive therapy even in the setting of chronic migraine [24]. Moreover, based on limited studies, topiramate has also been suggested to inhibit the progression of migraine in patients [25].

In this study we used a dose of NTG (10 mg/kg), which is substantially higher than the equivalent dose used to provoke migraine in humans [8]. It is therefore possible that this dose of NTG in mice could have additional effects apart from those associated with migraine induction in humans. The significant inhibition of NTG-induced hyperalgesia by systemic sumatriptan and topiramate, however, indicates that even if this dose of NTG represents a “supra-physiological” stimulus, it can nonetheless be effectively reversed by a standard dose of a proven acute migraine-specific therapy. Similarly, the ability of topiramate to inhibit the chronic basal hyperalgesia indicates that a standard migraine preventive therapy can reverse this component of the behavioral response.

Nitroglycerin evoked acute and chronic basal hyperalgesia is a promising mouse model for the investigation of migraine mechanisms and therapies. The enhancement of acute NTG-evoked hyperalgesia by a human migraine-associated gene expressed in mice, and the inhibition of this hyperalgesia by both acute and preventive migraine therapies provide strong support for the translational value of this model. Ongoing studies of the effects of other human migraine genes, as well as other established acute and preventive therapies, will help to further validate the model as a useful tool for enhancing our ability to understand and treat this frequently disabling disorder.

## Figure Legends

### **FIGURE 1**

Chronic NTG evokes and sustains mechanical hyperalgesia in a dose-dependent manner. C57Bl/6J mice were treated every second day with varying doses of NTG (0-10 mg/kg, ip) for 9 days. A) Increasing doses of NTG produced increasing levels of mechanical hyperalgesia, in mice tested 2 hours post-NTG or vehicle administration. n=8/group, p<0.001 effect of dose two-way RM ANOVA. (B) Basal mechanical responses, as assessed prior to vehicle or NTG administration, significantly decreased in the 3 and 10 mg/kg NTG group during the treatment period. n=8/group, p<0.001 effect of dose and time two-way RM ANOVA. Chronic NTG in rodents produces a dose-dependent persistent hypersensitivity.

### **FIGURE 2**

Chronic NTG evokes severe and sustained mechanical hyperalgesia. C57Bl/6J mice were treated every second day with vehicle (VEH) or NTG (10 mg/kg, ip) for 9 days. (A) NTG consistently produced severe mechanical hyperalgesia, in mice tested 2 hours post-NTG or vehicle administration. n=7-8/group, \*\*\*p<0.001 two-way RM ANOVA. (B) Basal mechanical responses, as assessed prior to vehicle or NTG administration, significantly decreased in the NTG group during the treatment period, and took 7 days to recover following the final NTG injection. n=7-8/group. (C) Females developed basal mechanical hyperalgesia more quickly than males following chronic NTG treatment. n=12/group, \*\*p<0.01 two-way RM ANOVA. Chronic NTG in rodents appears to model the persistent hypersensitivity observed in migraine patients.

**FIGURE 3** Sildenafil, a phosphodiesterase 5 inhibitor, potentiates hyperalgesia induced by a low dose of NTG. C57Bl/6J mice were treated every second day with vehicle (VEH) or a low dose

of NTG (1 mg/kg, ip) for 9 days. (A) Basal mechanical responses were assessed prior to NTG administration, n=8/group p<0.05 effect of drug and p<0.001 effect of time and interaction, two-way RM ANOVA. (B) Mice were injected ip with either vehicle (VEH) or 3 mg/kg sildenafil (SIL) 1h15min post-NTG administration, and tested 45min later (2h post-NTG). n=8/group, p<0.001 effect of drug, two-way RM ANOVA. Animals treated with both NTG and sildenafil showed significantly reduced basal and post-treatment responses.

#### FIGURE 4

Chronic NTG-evoked hyperalgesia is attenuated by systemic administration of sumatriptan. C57Bl/6J mice were treated every second day with NTG (10 mg/kg, ip) for 9 days. (A,B) Basal mechanical responses were assessed prior to NTG administration, and significantly and progressively decreased following the first treatment day. NTG injection produced further mechanical hyperalgesia (NTG-VEH), which was significantly attenuated by sumatriptan (B, 600 µg/kg, ip). Dashed line represents basal responses on day 1, n=5-6/group, \*p<0.05, \*\*p<0.01, \*\*\*p<0.001, 2-way RM ANOVA. (C) Intraplantar injection of CFA into the hindpaw produced significant hyperalgesia which was not affected by sumatriptan (600 µg/kg, ip). Dashed line represents baseline naïve mechanical responses before CFA injection, n=6/group. (D) Mice were injected with vehicle (VEH) or NTG (10 mg/kg, ip) and after 1h30min injected intrathecally with sumatriptan (0.06 µg in 5 µl) and tested 30min later. Dashed line represents basal responses prior to NTG injection. Pain produced by chronic NTG is alleviated by a systemically administered prototypic anti-migraine treatment.

#### FIGURE 5

Chronic treatment with the migraine prophylactic, topiramate, significantly attenuated NTG-induced basal and post-treatment hyperalgesia. C57Bl/6J mice were treated with vehicle (VEH) or topiramate (30 mg/kg ip) daily for 11 days. On days 3,5,7,9, and 11 baseline responses were

determined (A), and mice were injected with either vehicle (VEH) or NTG (10 mg/kg, ip). Post-treatment responses were assessed 2h following NTG administration. n=8/group, p<0.001 effect of NTG, two-way RM ANOVA. Both basal and acute hyperalgesia induced by chronic NTG can be alleviated by a well-characterized migraine preventative therapy.

## References

- [1] Stovner L, Hagen K, Jensen R, Katsarava Z, Lipton R, Scher A, Steiner T, Zwart JA. The global burden of headache: a documentation of headache prevalence and disability worldwide. *Cephalgia* 2007;27(3):193-210.
- [2] Bigal ME, Serrano D, Reed M, Lipton RB. Chronic migraine in the population: burden, diagnosis, and satisfaction with treatment. *Neurology* 2008;71(8):559-566.
- [3] Stewart WF, Wood C, Reed ML, Roy J, Lipton RB. Cumulative lifetime migraine incidence in women and men. *Cephalgia* 2008;28(11):1170-1178.
- [4] Victor TW, Hu X, Campbell JC, Buse DC, Lipton RB. Migraine prevalence by age and sex in the United States: a life-span study. *Cephalgia* 2010;30(9):1065-1072.
- [5] Iversen HK, Olesen J, Tfelt-Hansen P. Intravenous nitroglycerin as an experimental model of vascular headache. Basic characteristics. *Pain* 1989;38(1):17-24.
- [6] Christiansen I, Thomsen LL, Daugaard D, Ulrich V, Olesen J. Glyceryl trinitrate induces attacks of migraine without aura in sufferers of migraine with aura. *Cephalgia* 1999;19(7):660-667.
- [7] Afridi SK, Matharu MS, Lee L, Kaube H, Friston KJ, Frackowiak RS, Goadsby PJ. A PET study exploring the laterality of brainstem activation in migraine using glyceryl trinitrate. *Brain* 2005;128(Pt 4):932-939.
- [8] Olesen J. The role of nitric oxide (NO) in migraine, tension-type headache and cluster headache. *Pharmacol Ther* 2008;120(2):157-171.
- [9] Olesen J. Nitric oxide-related drug targets in headache. *Neurotherapeutics : the journal of the American Society for Experimental NeuroTherapeutics* 2010;7(2):183-190.
- [10] Bates EA, Nikai T, Brennan KC, Fu YH, Charles AC, Basbaum AI, Ptacek LJ, Ahn AH. Sumatriptan alleviates nitroglycerin-induced mechanical and thermal allodynia in mice. *Cephalgia* 2010;30(2):170-178.
- [11] Markovics A, Kormos V, Gaszner B, Lashgarara A, Szoke E, Sandor K, Szabadfi K, Tuka B, Tajti J, Szolcsanyi J, Pinter E, Hashimoto H, Kun J, Reglodi D, Helyes Z. Pituitary adenylate cyclase-activating polypeptide plays a key role in nitroglycerol-induced trigeminovascular activation in mice. *Neurobiol Dis* 2012;45(1):633-644.
- [12] Brennan KC, Bates EA, Shapiro RE, Zyuzin J, Hallows WC, Huang Y, Lee HY, Jones CR, Fu YH, Charles AC, Ptacek LJ. Casein kinase idelta mutations in familial migraine and advanced sleep phase. *Science translational medicine* 2013;5(183):183ra156.
- [13] Greco R, Meazza C, Mangione AS, Allena M, Bolla M, Amantea D, Mizoguchi H, Sandrini G, Nappi G, Tassorelli C. Temporal profile of vascular changes induced by systemic nitroglycerin in the meningeal and cortical districts. *Cephalgia* 2011;31(2):190-198.
- [14] Zimmermann M. Ethical guidelines for investigations of experimental pain in conscious animals. *Pain* 1983;16(2):109-110.
- [15] Nikai T, Basbaum AI, Ahn AH. Profound reduction of somatic and visceral pain in mice by intrathecal administration of the anti-migraine drug, sumatriptan. *Pain* 2008;139(3):533-540.
- [16] Chaplan SR, Bach FW, Pogrel JW, Chung JM, Yaksh TL. Quantitative assessment of tactile allodynia in the rat paw. *JNeurosciMethods* 1994;53(1):55-63.
- [17] Schoonman GG, van der GJ, Kortmann C, van der Geest RJ, Terwindt GM, Ferrari MD. Migraine headache is not associated with cerebral or meningeal vasodilatation--a 3T magnetic resonance angiography study. *Brain* 2008;131(Pt 8):2192-2200.

- [18] Greco R, Tassorelli C, Mangione AS, Smeraldi A, Allena M, Sandrini G, Nappi G, Nappi RE. Effect of sex and estrogens on neuronal activation in an animal model of migraine. Headache 2013;53(2):288-296.
- [19] Bigal ME, Lipton RB. Excessive acute migraine medication use and migraine progression. Neurology 2008;71(22):1821-1828.
- [20] Edelmayer RM, Ossipov MH, Porreca F. An experimental model of headache-related pain. Methods in molecular biology (Clifton, NJ) 2012;851:109-120.
- [21] Edelmayer RM, Le LN, Yan J, Wei X, Nassini R, Materazzi S, Preti D, Appendino G, Geppetti P, Dodick DW, Vanderah TW, Porreca F, Dussor G. Activation of TRPA1 on dural afferents: a potential mechanism of headache pain. Pain 2012;153(9):1949-1958.
- [22] Burstein R, Jakubowski M, Garcia-Nicas E, Kainz V, Bajwa Z, Hargreaves R, Becerra L, Borsook D. Thalamic sensitization transforms localized pain into widespread allodynia. Annals of neurology 2010;68(1):81-91.
- [23] Mullenens WM, Chronicle EP. Anticonvulsants in migraine prophylaxis: a Cochrane review. Cephalgia 2008;28(6):585-597.
- [24] Diener HC, Bussone G, Van Oene JC, Lahaye M, Schwalen S, Goadsby PJ. Topiramate reduces headache days in chronic migraine: a randomized, double-blind, placebo-controlled study. Cephalgia 2007;27(7):814-823.
- [25] Limmroth V, Biondi D, Pfeil J, Schwalen S. Topiramate in patients with episodic migraine: reducing the risk for chronic forms of headache. Headache 2007;47(1):13-21.

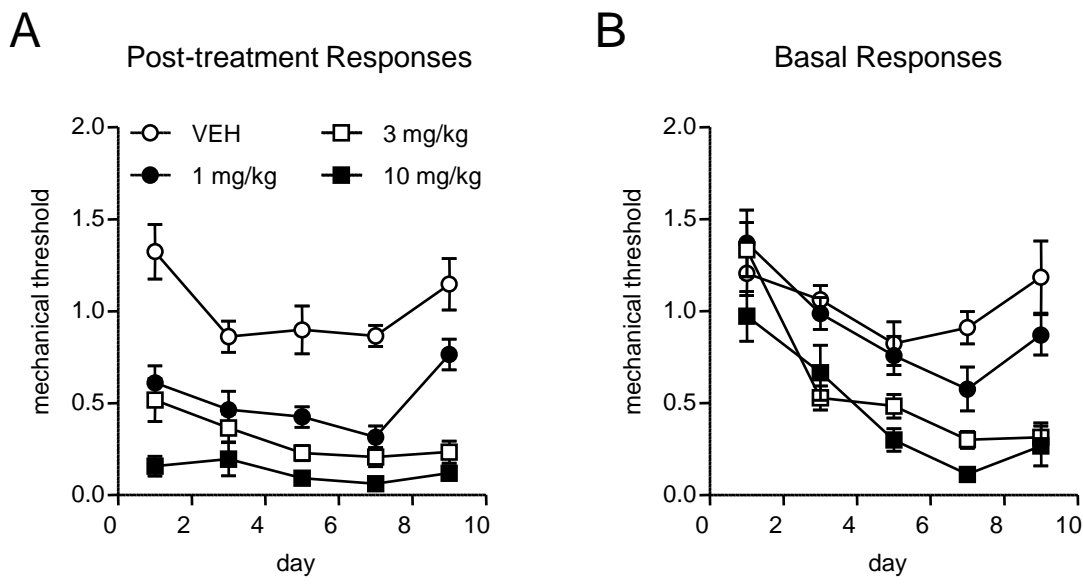


Figure 1 Pradhan et al.

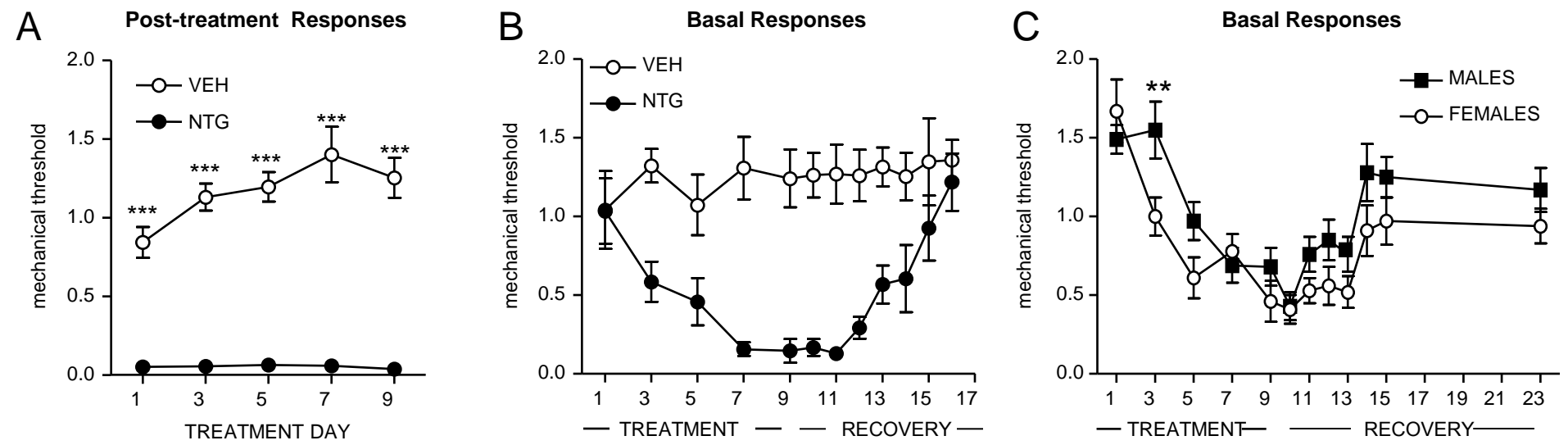
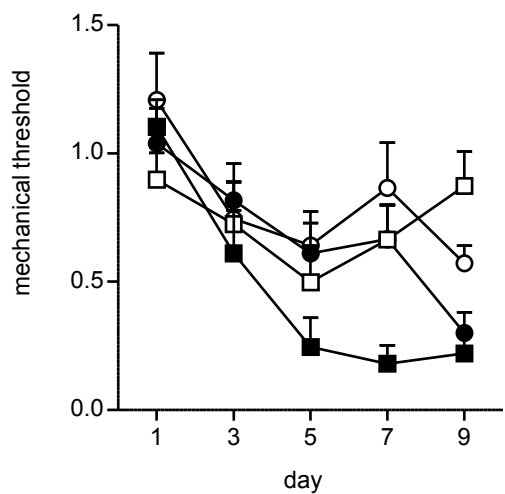


Figure 2 Pradhan et al.

**A**

## Basal Responses

**B**

## Post-treatment Responses

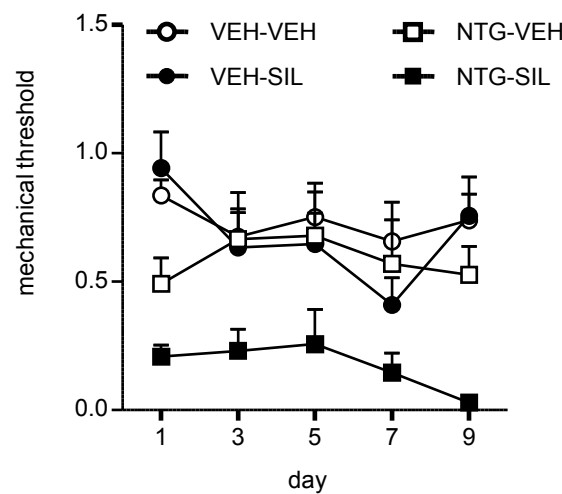
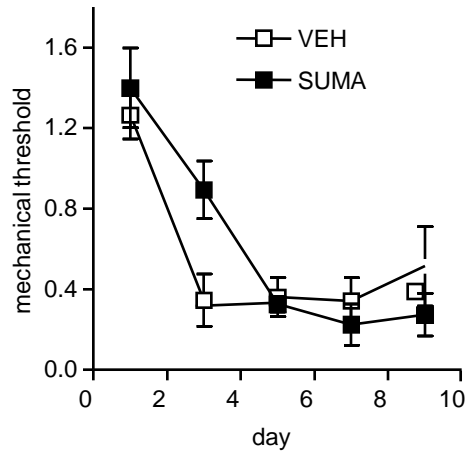


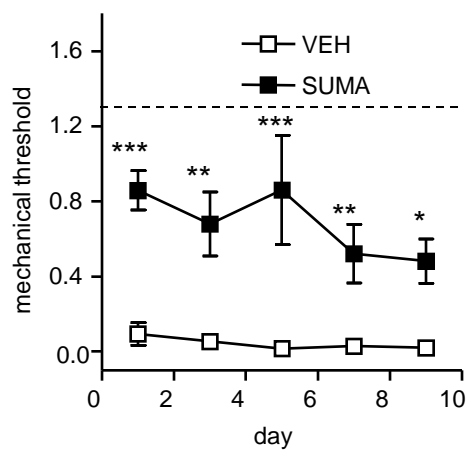
Figure 3 Pradhan et al.

**A**

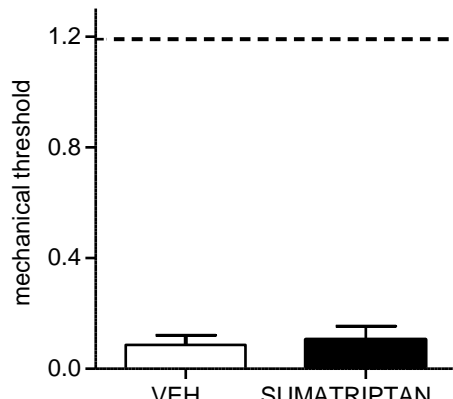
## Basal Responses

**B**

## Post-treatment Responses

**C**

## Inflammatory Pain

**D**

## Intrathecal Injection

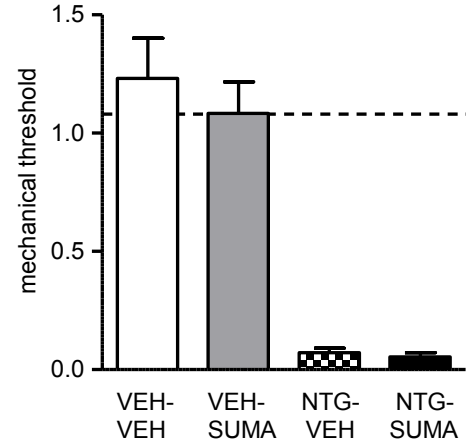


Figure 4 Pradhan et al.

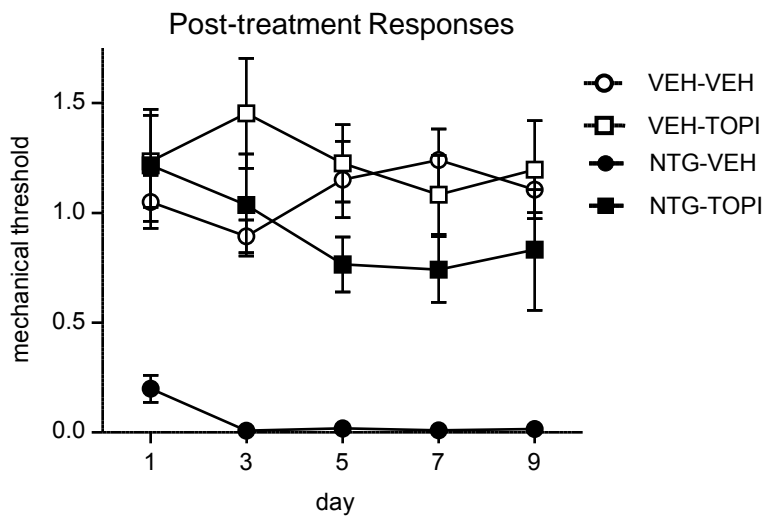
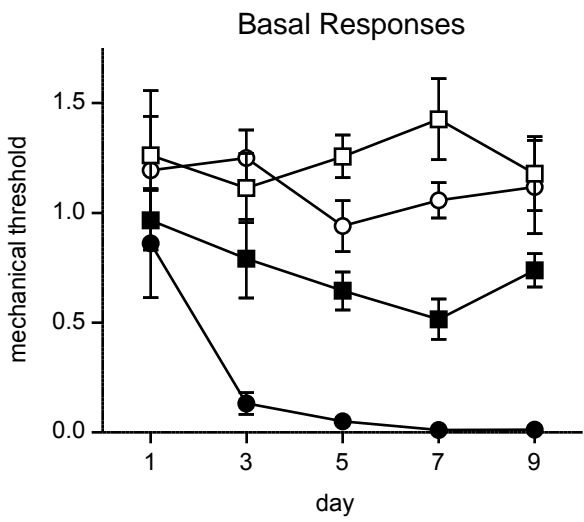


Figure 5 Pradhan et al.

## MIGRAINE

# Casein Kinase I $\delta$ Mutations in Familial Migraine and Advanced Sleep Phase

K. C. Brennan,<sup>1,2\*</sup> Emily A. Bates,<sup>3,4\*</sup> Robert E. Shapiro,<sup>5\*</sup> Jekaterina Zyuzin,<sup>1</sup> William C. Hallows,<sup>3</sup> Yong Huang,<sup>3</sup> Hsien-Yang Lee,<sup>3</sup> Christopher R. Jones,<sup>2</sup> Ying-Hui Fu,<sup>3</sup> Andrew C. Charles,<sup>1†</sup> Louis J. Ptáček<sup>3,6†</sup>

Migraine is a common disabling disorder with a significant genetic component, characterized by severe headache and often accompanied by nausea, vomiting, and light sensitivity. We identified two families, each with a distinct missense mutation in the gene encoding casein kinase I $\delta$  (CKI $\delta$ ), in which the mutation cosegregated with both the presence of migraine and advanced sleep phase. The resulting alterations (T44A and H46R) occurred in the conserved catalytic domain of CKI $\delta$ , where they caused reduced enzyme activity. Mice engineered to carry the CKI $\delta$ -T44A allele were more sensitive to pain after treatment with the migraine trigger nitroglycerin. CKI $\delta$ -T44A mice also exhibited a reduced threshold for cortical spreading depression (believed to be the physiological analog of migraine aura) and greater arterial dilation during cortical spreading depression. Astrocytes from CKI $\delta$ -T44A mice showed increased spontaneous and evoked calcium signaling. These genetic, cellular, physiological, and behavioral analyses suggest that decreases in CKI $\delta$  activity can contribute to the pathogenesis of migraine.

## INTRODUCTION

Migraine is a complex neurological disorder that affects 20 to 30% of the population (1, 2). About one-third of patients with migraine experience aura: a visual, sensory, or language disturbance preceding the migraine headache (3). Family and epidemiological studies provide strong evidence for a genetic contribution to migraine, although environmental factors also play a role (4, 5). Mutations in three different genes have been identified to cause familial hemiplegic migraine, an uncommon variant of migraine associated with unilateral weakness (6–8). The genetic basis for common forms of migraine (with and without aura) is less clear. Multiple susceptibility loci for migraine have been identified (9–12), and a potassium channel gene has been linked to migraine with aura in a single family (13). These studies suggest that a variety of genetic alterations affecting various aspects of brain excitability can lead to similar migraine phenotypes.

Here, we describe a family that presented for clinical evaluation of familial migraine with aura. In addition to migraine, the family members exhibited circadian patterns consistent with familial advanced sleep phase syndrome (FASPS), in which individuals go to sleep unusually early in the evening and wake early in the morning. We identified a mutation (threonine to alanine, T44A) in casein kinase I $\delta$  (CKI $\delta$ ) as a cause of FASPS in this family (14). CKI $\delta$  is a ubiquitous serine-threonine kinase that phosphorylates the circadian clock protein Per2 and many other proteins involved in brain signaling (15). In vitro studies showed that the T44A alteration in CKI $\delta$  resulted in reduced enzyme function in vitro, and both mice and flies expressing the mutant allele had significant sleep-wake cycle alterations (14). Given that migraine with aura was a prominent component of the presenting phenotype

of the family in whom the CKI $\delta$  mutation was identified, we investigated a potential role for CKI $\delta$  in migraine.

## RESULTS

### Human phenotypes

Fourteen members of the initial family with CKI $\delta$  allele-associated FASPS (K5231) were available for structured interview, physical examination, and CKI $\delta$  genotyping, including four spouses of affected individuals with potentially affected offspring (Fig. 1A). The proband (#33376) carried the CKI $\delta$ -T44A allele and met diagnostic criteria both for FASPS and for migraine with aura (MA) by ICHD-2 (International Classification of Headache Disorders, Second Edition) criteria (16). Of the 13 other family members that we characterized, 5 individuals carried the CKI $\delta$ -T44A allele, and all of these also met diagnostic criteria for either MA or migraine without aura (MO). Three individuals who were offspring of CKI $\delta$ -T44A allele carriers, but did not carry the allele themselves, also met diagnostic criteria for MA (Fig. 1A).

The clinical characteristics of migraine for the CKI $\delta$ -T44A allele carriers were unremarkable with respect to age of onset, time of day of attack onset, duration and character of aura symptoms, presence of cutaneous allodynia (the experience of innocuous touch as uncomfortable or tender), and duration of headache per attack. The proband (#33376) developed chronic migraine (more than 15 headache days per month) from her early 20s through her early 30s and then again between her early 40s and her early 50s with spontaneous remission each time. Brain magnetic resonance imaging studies for three individuals (#33373, #33374, and #33376) were unremarkable apart from evidence of a previous pituitary tumor excision in #33373. The proband's mother (#33374) had French-Canadian ancestry.

After identifying CKI $\delta$ -T44A in K5231, we sequenced the gene encoding CKI $\delta$  in blood samples from more than 70 FASPS probands and identified a second mutation in a single individual (#35315 in kindred 5579) that predicts a histidine-to-arginine change at position 46 (H46R) (Fig. 1B and fig. S1), two amino acids downstream from

<sup>1</sup>Department of Neurology, University of California, Los Angeles, Los Angeles, CA 90095, USA.

<sup>2</sup>Department of Neurology, University of Utah, Salt Lake City, UT 84108, USA. <sup>3</sup>Department of Neurology, University of California, San Francisco, San Francisco, CA 94158, USA. <sup>4</sup>Department of Chemistry and Biochemistry, Brigham Young University, Provo, UT 84602, USA. <sup>5</sup>Department of Neurological Sciences, University of Vermont, Burlington, VT 05401, USA. <sup>6</sup>Howard Hughes Medical Institute, University of California, San Francisco, San Francisco, CA 94158, USA.

\*These authors contributed equally to this work.

†Corresponding author. E-mail: acharles@ucla.edu (A.C.C.); ljp@ucsf.edu (L.J.P.)

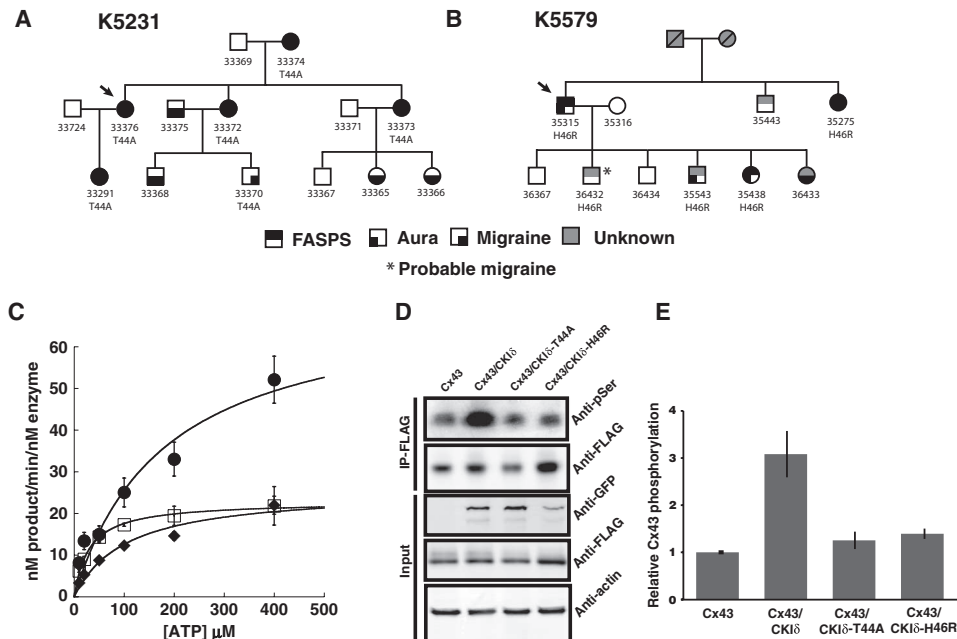


**Fig. 1. Migraine kindreds with mutations in the gene encoding CKI $\delta$  and in vitro enzymatic analysis.** (A) Kindred 5231 segregating the T44A CKI $\delta$  allele. (B) Kindred 5579 segregating the H46R CKI $\delta$  allele. Phenotypes are as noted, and probands are indicated by arrows. “Migraine” indicates symptoms consistent with ICHD-2 migraine without aura. “Aura” indicates symptoms consistent with ICHD-2 migraine aura. (C) Saturation kinetic analysis of wild-type (●), T44A (□), and H46R (◆) CKI $\delta$  $\Delta$ 317 using  $\alpha$ -casein, PER2 peptide, and ATP. (D and E) Phosphorylation assays. Transiently transfected connexin43 is phosphorylated when coexpressed with CKI $\delta$  wild type. FLAG-connexin43 was expressed alone or with CKI $\delta$  wild type, T44A, and H46R in HEK293 cells. FLAG-connexin43 was immunoprecipitated by anti-FLAG conjugated to agarose at 4°C for 4 hours. These extracts were resolved by SDS-polyacrylamide gel electrophoresis (SDS-PAGE), and phosphorylated and dephosphorylated connexin43 was detected by Western blotting with anti-phosphoserine and anti-FLAG antibodies, respectively. Input blot proteins were detected with anti-FLAG, anti-GFP (green fluorescent protein), and  $\beta$ -actin antibody. Relative phosphorylation was normalized to connexin43 protein levels, quantified, and analyzed by LI-COR image software. Data are means  $\pm$  SEM ( $n \geq 4$ ). \* $P < 0.05$ , analysis of variance (ANOVA) followed by Tukey test.

the T44A substitution. This family is primarily of English and Irish descent. Information regarding the migraine phenotype in the family with the H46R mutation was obtained by an e-mail survey and by follow-up e-mail or phone contact. Phenotypic data were analyzed blind to genotypes and FASPS phenotypes. Four of the five family members who carried the H46R allele had MO, MA, or migraine aura without headache, and the fifth had probable migraine by ICHD-2 criteria. Of five family members who did not carry the H46R allele, one had MA. We examined the 1000 Genomes database, National Heart, Lung, and Blood Institute (NHLBI) ESP6500 variant data set, and 69 public genomes from Complete Genomics for the T44A and H46R alleles that we had identified in the migraine families and found neither allele in these controls. No other coding variants in the first 200 amino acids of CKI $\delta$  were found in Caucasian samples available in public databases. We also sequenced DNA from an additional 250 Northern European controls from our laboratories and found these alleles in none of them. Furthermore, the protein sequences of CKI $\delta$  are extremely conserved across species from human to fruit fly to single-cell algae, and T44 and H46 are absolutely conserved (fig. S1). Thus, these two CKI $\delta$  alleles were not present in more than 2600 control chromosomes. We estimate that the chances of coincidentally having mutations in the same

ultraconserved region in two families with the same phenotype are extremely small.

We previously showed that the CKI $\delta$ -T44A protein has reduced kinase activity in comparison to the wild-type enzyme (14). We repeated these experiments for the CKI $\delta$ -H46R isoform (Fig. 1C). CKI $\delta$ -H46R also showed decreased kinase activity with a  $V_{max}$  of (mean  $\pm$  SEM)  $104.64 \pm 6.61$  nM min $^{-1}$  nM $^{-1}$  compared to  $198.27 \pm 11.23$  nM min $^{-1}$  nM $^{-1}$  for the wild-type enzyme, representing a 53% reduction in activity ( $P < 0.01$ ,  $n = 3$ ). The Michaelis constant ( $K_m$ ) was  $43.38 \pm 6.17$   $\mu$ M for CKI $\delta$ -H46R and  $36.48 \pm 7.79$   $\mu$ M for wild-type CKI $\delta$  (Table 1). This decrease in  $V_{max}$  suggests that the mutation causes a reduction in the catalytic rate of phosphotransfer. There may be a subtle effect on enzyme recognition of the substrate as the  $K_m$  of the mutant kinase activity is decreased with PER2 peptide but is not significantly different with casein or adenosine triphosphate (ATP). We also tested the ability of wild-type and mutant forms of CKI $\delta$  to phosphorylate connexin43, a known substrate hypothesized to be relevant to migraine (17). Both the T44A and H46R mutant forms of CKI $\delta$  phosphorylated connexin43 to a lesser degree than did wild-type CKI $\delta$  (Fig. 1, D and E).

### Increased nitroglycerin-induced hyperalgesia in CKI $\delta$ -T44A mice

To further examine whether mutant CKI $\delta$  can cause migraine symptoms, we tested CKI $\delta$ -T44A transgenic mice for their susceptibility to a migraine-like phenotype.

Nitroglycerin (NTG) evokes peripheral mechanical and thermal hyperalgesia in mice and humans (18, 19). We quantified NTG-evoked mechanical and thermal hyperalgesia in CKI $\delta$ -T44A mice and wild-type littermate controls. Mechanical and thermal nociception thresholds were determined with von Frey filaments and the Hargreaves radiant heat assay, before and for a 4-hour period after intraperitoneal injection of NTG (1, 3, 5, 7, or 10 mg/kg). During the 4-hour follow-up, the mechanical thresholds were significantly lower in CKI $\delta$ -T44A mice than in wild-type controls ( $n = 14$  wild-type and 15 CKI $\delta$ -T44A,  $P < 0.01$  for each dose with a linear mixed-effects model; Fig. 2 and table S1). After NTG injection, CKI $\delta$ -T44A mice were also more sensitive to thermal stimuli than wild-type siblings, with a significantly slower recovery from thermal hyperalgesia ( $n = 24$  CKI $\delta$ -T44A and  $n = 21$  wild-type mice;  $P < 0.01$  for each dose with a linear mixed-effects model; Fig. 2 and table S2). Because migraine is more common in women than men, we compared female and male CKI $\delta$ -T44A mice with wild-type animals 90 min after NTG (5 mg/kg) injection. At this dose and time point, female, but not male, CKI $\delta$ -T44A mice showed a significant reduction in latency to paw withdrawal compared to wild-type animals (males: wild-type,  $0.99 \pm 0.69$  s; CKI $\delta$ -T44A,  $2.46 \pm 0.7$  s;  $P = 0.38$ ; females: wild-type,  $0.69 \pm 0.75$  s; CKI $\delta$ -T44A,  $2.87 \pm 0.58$  s;  $P = 0.008$ ,

**Table 1. Biochemical characterization of the migraine-associated CKI $\delta$  mutant enzymes.**  $n \geq 3$  independent experiments with three replicates each; all measurements shown are  $\pm$ SEM.

Substrate	$\alpha$ -Casein		PER2 peptide		ATP	
	$V_{max}$ (nM min $^{-1}$ nM $^{-1}$ )	$K_m$ ( $\mu$ M)	$V_{max}$ (nM min $^{-1}$ nM $^{-1}$ )	$K_m$ ( $\mu$ M)	$V_{max}$ (nM min $^{-1}$ nM $^{-1}$ )	$K_m$ ( $\mu$ M)
Wild-type CKI $\delta$ Δ317	198.3 $\pm$ 11.2	36.5 $\pm$ 6.2	184.0 $\pm$ 24.4	635.8 $\pm$ 131.4	71.7 $\pm$ 14.7	180.6 $\pm$ 80.1
CKI $\delta$ -T44AΔ317	130.3 $\pm$ 6.7*	29.4 $\pm$ 4.8	80.1 $\pm$ 12.6*	230.6 $\pm$ 76.5*	22.9 $\pm$ 0.4*	30.0 $\pm$ 2.2
CKI $\delta$ -H46RAΔ317	104.6 $\pm$ 6.6*	43.4 $\pm$ 7.8	49.5 $\pm$ 8.8*	371 $\pm$ 120.4*	25.8 $\pm$ 3.2*	104.7 $\pm$ 33.3

\* $P < 0.05$  (Student's *t* test).

ANOVA with post hoc Tukey test), suggesting that both sex and genotype may contribute to the difference in thermal hyperalgesia. Rotarod testing showed no difference in initial or repeat performance for CKI $\delta$ -T44A mice and wild-type mice (fig. S2), suggesting that differences in response to thermal and mechanical stimulation were not due to differences in motor function or learning.

Neurons in the trigeminal nucleus caudalis (TNC) and laminae I to V of upper cervical dorsal horn (C1 and C2) receive craniofacial pain input and are believed to be activated during migraine (20–23). We administered NTG (5 mg/kg) to CKI $\delta$ -T44A ( $n = 7$ ) and wild-type littermates ( $n = 6$ ) and measured the number of activated neurons in TNC, C1, and C2 with Fos immunohistochemistry. After NTG treatment, we found a significant increase in the number of Fos-positive nuclei in all three areas in CKI $\delta$ -T44A animals compared to wild-type littermates in TNC (mean  $\pm$  SEM, 34  $\pm$  2 versus 11  $\pm$  1), C1 dorsal horn (33  $\pm$  3 versus 17  $\pm$  2), and C2 dorsal horn (28  $\pm$  2 versus 14  $\pm$  2) (Fig. 3). The number of Fos-positive nuclei was not significantly different in laminae VI to X.

### Reduced threshold for induction of cortical spreading depression in CKI $\delta$ -T44A mice

To investigate the effects of CKI $\delta$  mutations on migraine-related cortical excitability, we used optical imaging and electrophysiological recording to measure cortical spreading depression (CSD) in vivo in CKI $\delta$ -T44A mice (Fig. 4, A and B). Potassium chloride (KCl) was applied to the cortex at increasing volumes until CSD was induced to determine the threshold for evoking CSD (24). CSD thresholds were significantly lower in CKI $\delta$ -T44A compared to wild-type mice (Fig. 4D). CSD velocities were similar in both groups (Fig. 4C). After we determined these threshold values, repeat inductions were performed at threshold stimulus every 10 min

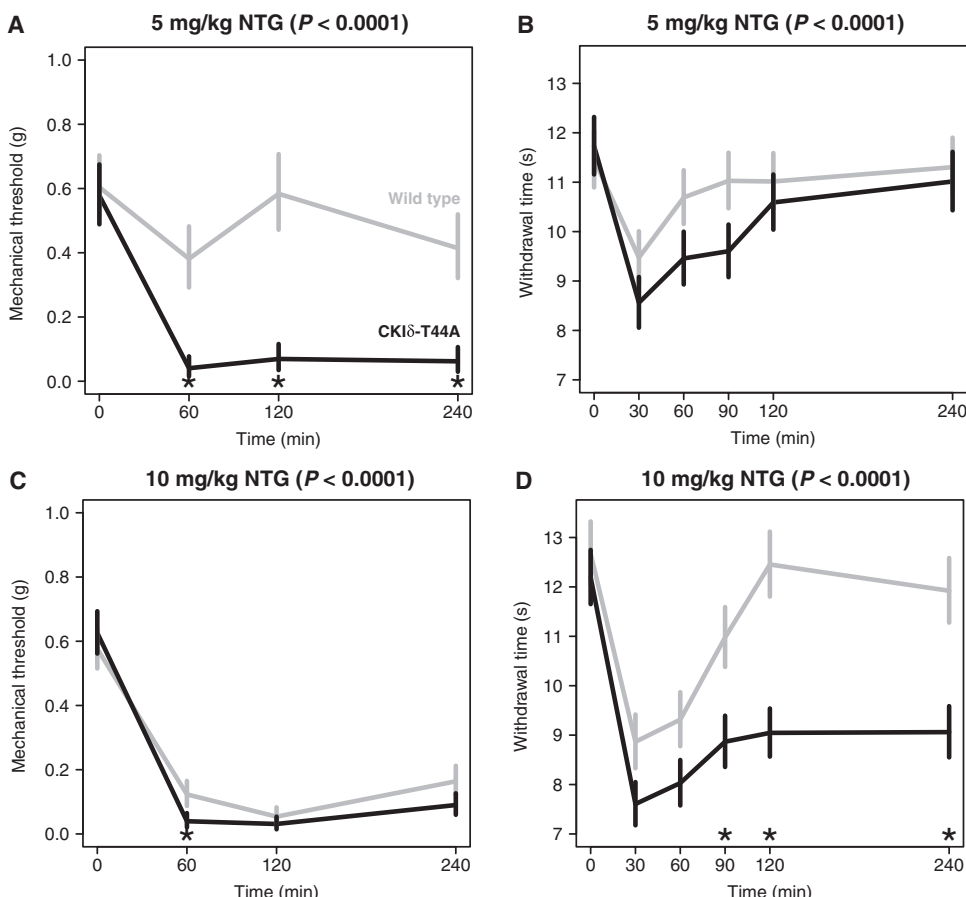


**Fig. 2. Differential effects of mechanical and thermal stimuli in response to NTG for wild-type and CKI $\delta$ -T44A mice.** Data shown (means  $\pm$  SEM) were compared with a linear mixed-effects model. Gray lines, wild type; black lines, CKI $\delta$ -T44A. Differences across time between CKI $\delta$ -T44A and wild type are significant at each NTG dosage ( $P$  values displayed for each panel). Asterisks indicate time points with significant difference between genotypes. (A and C) Mechanical hyperalgesia measured with von Frey hair (Semmes-Weinstein monofilament). (B and D) Thermal hyperalgesia in CKI $\delta$ -T44A and wild-type mice in response to NTG [5 mg/kg (B) or 10 mg/kg (D)] intraperitoneal injection, measured with radiant heat assay (Hargreaves test). \* $P < 0.05$  (see tables S1 and S2 for detailed data).

for the next 60 min. Despite the difference in the thresholds, there was no significant difference in the number of successful CSD inductions between the two groups (Fig. 4), showing that the lower CSD thresholds in CKI $\delta$ -T44A mice were reproducible over time. The number of CSDs induced in response to a constant stimulus is also used to

measure CSD susceptibility (25). During 60 min of continuous application of KCl, CKI $\delta$ -T44A mice showed a significantly greater number of CSD events than did wild-type mice (Fig. 4E).

### Enhanced CSD-associated arterial dilation in CKI $\delta$ -T44A mice

Meningeal and cortical surface arteries react to CSD (26, 27). Activation of perivascular nociceptive afferents has been proposed as a mechanism through which CSD activates the TNC (21, 23). Pre-CSD baseline arterial diameter was the same in CKI $\delta$ -T44A and wild-type mice (Fig. 5). In both CKI $\delta$ -T44A and wild-type mice, CSD was associated with multiphasic changes in arterial diameter: an initial dilation coincident with or ahead of the CSD wavefront, a constriction corresponding to the tissue depolarization, and a second dilation before a return toward baseline (27) (Fig. 5). Cortical surface arteries were more dilated in all phases of CSD in CKI $\delta$ -T44A mice compared with wild-type mice (Fig. 5C). We found no correlation between the magnitude of CSD-associated changes in vascular caliber and CSD threshold (177 diameter measurements in 15 mice where such measurement was possible: dilation 1:  $r = -0.009$ ,  $t = 0.11$ ,  $t_{\text{crit}} = 1.97$ ,  $P = 0.9$ ; constriction:  $r = 0.11$ ,  $P = 0.13$ ; dilation 2:  $r = 0.02$ ,  $P = 0.69$ ; post-CSD baseline:  $r = -0.006$ ,  $P = 0.92$ ), suggesting that these vascular differences were not due to the lower CSD thresholds in CKI $\delta$ -T44A mice.

**Amplitude, duration, and velocity of CSD.** We compared the amplitude and duration of both intrinsic signal and electrophysiological variables associated with CSD in CKI $\delta$ -T44A and wild-type mice (table S3). There was no significant difference in intrinsic signal or dc (direct current) shift amplitude. Although the durations of intrinsic signal changes and dc shifts were significantly shorter in CKI $\delta$ -T44A mice, there was a significant correlation between duration of dc shift and CSD threshold in all mice ( $r = 0.6$ ,  $t = 3.83$ ,  $t_{\text{crit}} = 2.05$ ,  $P = 0.0007$ ,  $n = 25$  mice) and in CKI $\delta$ -T44A and wild-type mice considered separately (CKI $\delta$ -T44A:  $r = 0.56$ ,  $t = 2.68$ ,  $t_{\text{crit}} = 2.13$ ,  $P = 0.02$ ,  $n = 17$  mice; wild type:  $r = 0.65$ ,  $t = 2.56$ ,  $t_{\text{crit}} = 1.83$ ,  $P = 0.03$ ) (fig. S4). We ascribed this difference in duration to the significant difference in thresholds between the two groups. The velocity of CSD was similar between CKI $\delta$ -T44A and wild-type mice, with no significant difference detected (Fig. 4C).

**Sex differences in CSD susceptibility.** We previously identified a reduced threshold for CSD in female compared to male C57Bl/6 mice (24), and others have found a reduced CSD threshold in female mice expressing familial hemiplegic migraine mutations (28). We observed a gradient of CSD thresholds by sex and genotype, with the lowest thresholds in female CKI $\delta$ -T44A and the highest in male wild-type animals (fig. S3). ANOVA analysis of CSD thresholds by gender and genotype revealed a significant difference over the four combinations (female CKI $\delta$ -T44A, male CKI $\delta$ -T44A, female wild-type, and male wild-type; one-way ANOVA,  $F = 3.74$ ,  $F_c = 2.70$ ,  $P = 0.01$ ). Post hoc Tukey test showed that the only significantly different paired comparison was between female CKI $\delta$ -T44A and male wild-type mice. We concluded that, although there may be a trend toward sex differences in our data set, the main driver of differences was genotype.

### Calcium signaling in astrocytes from CKI $\delta$ -T44A mice

Astrocyte Ca<sup>2+</sup> signaling occurs in conjunction with CSD and may mediate some of the vascular changes associated with CSD (29). The primary connexin expressed by astrocytes, connexin43, is a mediator of astrocyte signaling and can be modulated by CKI $\delta$  (30). We found that a greater number of cultured astrocytes from CKI $\delta$ -T44A mice

showed spontaneous Ca<sup>2+</sup> oscillations and intercellular Ca<sup>2+</sup> waves than did astrocytes from wild-type mice (Fig. 6). We also investigated the effects of exposure to medium without extracellular Ca<sup>2+</sup> (0 Ca<sup>2+</sup>), a condition that evokes intercellular waves of increased intracellular Ca<sup>2+</sup> in astrocytes by causing release of ATP (31, 32). Astrocytes from CKI $\delta$ -T44A mice showed an increased Ca<sup>2+</sup> response to 0 Ca<sup>2+</sup> medium compared to wild-type astrocytes, with a greater number of sites of initiation of intercellular Ca<sup>2+</sup> waves and a greater extent of propagation of intercellular Ca<sup>2+</sup> waves (Fig. 6, B and C). We did not, however, detect a significant increase in ATP release to this stimulus in astrocytes from CKI $\delta$ -T44A mice (fig. S5).

### DISCUSSION

We identified two distinct missense mutations in the gene encoding CKI $\delta$  that cosegregated with migraine in two independent families with

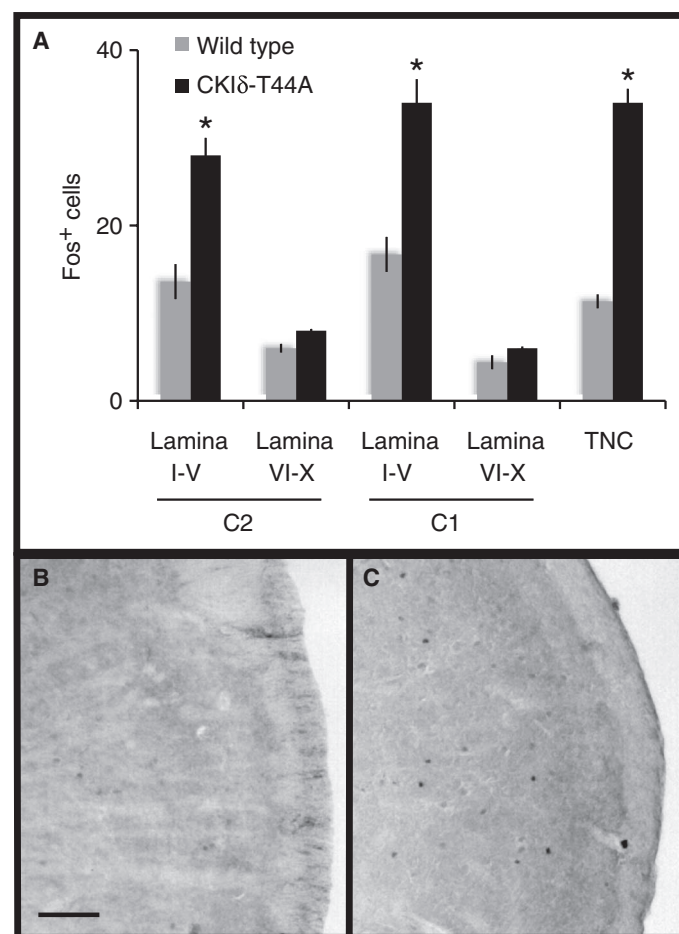


**Fig. 3. NTG-induced Fos expression in the spinal cord and TNC.** (A) Quantification of Fos-immunoreactive nuclei in the cervical spinal cord lamina I to V, VI to X, and TNC in age-matched wild-type ( $n = 6$ ) and CKI $\delta$ -T44A transgenic ( $n = 7$ ) mice 2 hours after treatment with systemic NTG (5 mg/kg). Data are expressed as average numbers of Fos<sup>+</sup> cells per section. \* $P < 1 \times 10^{-5}$ , two-way Student's *t* test. (B and C) Representative sections showing Fos immunoreactivity in wild-type (B) and CKI $\delta$ -T44A (C) TNC.

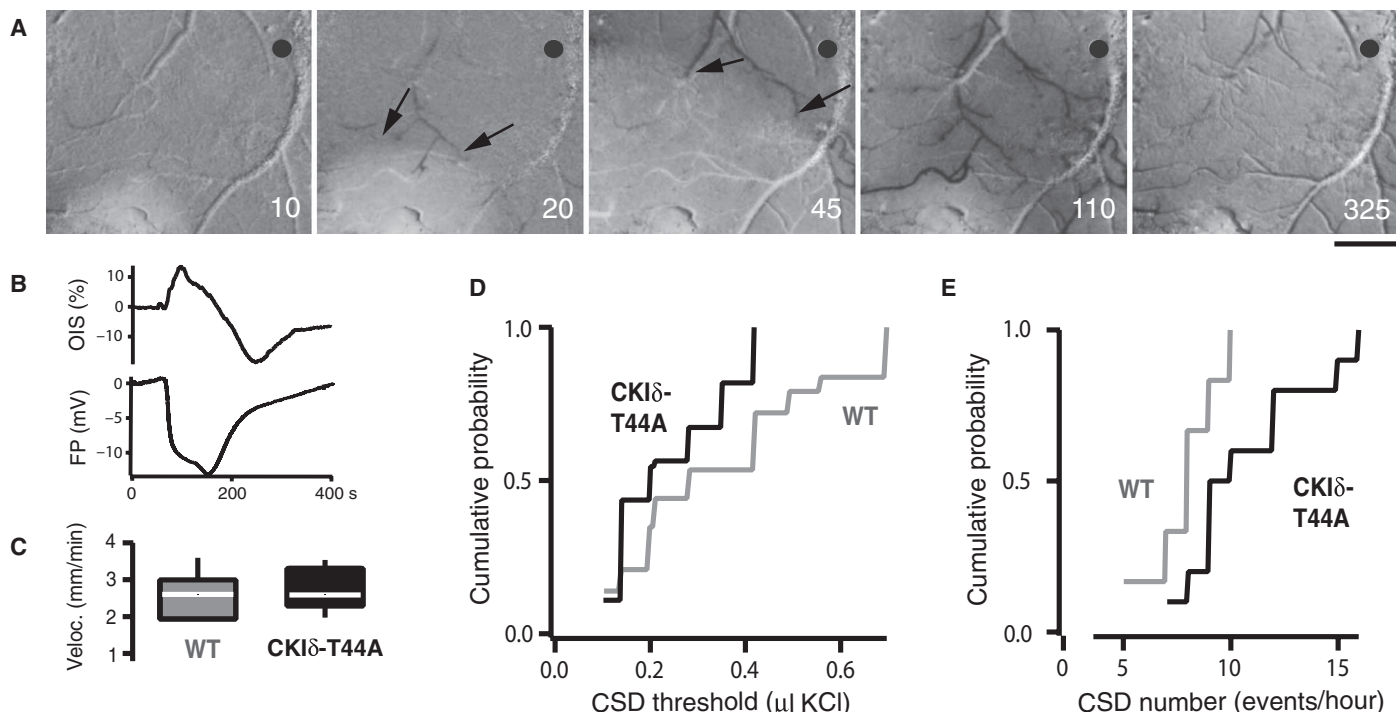


**Fig. 4. Increased susceptibility to CSD in CKI $\delta$ -T44A mice.** (A) Normalized reflectance images ( $r/r_0 \times 100$ ) show CSD-associated optical intrinsic signal (OIS) changes in a CKI $\delta$ -T44A mouse brain. KCl-induced CSD causes changes in reflectance that propagate concentrically outward from the source at about 3 mm/min. Reduced reflectance precedes brightening, followed by profound darkening (image 4) before return toward baseline. Reduced arterial reflectance shows the arterial dilation (arrows) that precedes CSD. Numbers indicate the seconds after CSD induction. Scale bar, 500  $\mu$ m. Gray circle, field potential electrode and optical measurement location. (B) OIS and field potential traces from the same experiment as in (A), showing OIS changes and the direct current field potential shift of CSD. OIS trace shows percentage change from pre-CSD. (C) CSD velocity in CKI $\delta$ -T44A mice and wild-type (WT) littermates. Median [interquartile range (IQR)] velocity was 2.7 mm/min (2.0 to 3.0 mm/min) in wild-type littermates

and 2.6 mm/min (2.3 to 3.2 mm/min) in CKI $\delta$ -T44A mice ( $n = 6$  wild-type mice, 17 CSD; 9 CKI $\delta$ -T44A mice, 29 CSD;  $P = 0.77$ , Mann-Whitney-Wilcoxon test). (D) Threshold for CSD in wild-type and CKI $\delta$ -T44A mice. Median (IQR) threshold was 0.28  $\mu$ l (0.2 to 0.49  $\mu$ l) of 1 M KCl in wild-type littermates compared to 0.20  $\mu$ l (0.14 to 0.35  $\mu$ l) for CKI $\delta$ -T44A mice ( $n = 11$  wild-type mice, 43 CSDs; 14 CKI $\delta$ -T44A mice, 55 CSDs;  $P = 0.001$ , Mann-Whitney-Wilcoxon test). There was no significant difference in the ratio of successful CSD inductions in wild-type (3.90:6) versus CKI $\delta$ -T44A (3.92:6) mice ( $n = 11$  wild-type, 14 CKI $\delta$ -T44A mice;  $P = 0.34$ , Mann-Whitney-Wilcoxon test). (E) Elicitation of CSD in response to constant stimulation over an hour in CKI $\delta$ -T44A mice and their wild-type littermates. Wild-type mice had median (IQR) of 8.0 CSD/hour (6.5 to 9.25 CSD/hour) and CKI $\delta$ -T44A mice had 9.5 CSD/hour (8.75 to 12.75 CSD/hour) ( $n = 6$  wild-type mice, 10 CKI $\delta$ -T44A mice;  $P = 0.03$ , Mann-Whitney-Wilcoxon test).

advanced sleep phase syndrome. The mutations (T44A and H46R) occur in a conserved catalytic domain and reduce CKI $\delta$  kinase activity compared to wild-type. Mice expressing the CKI $\delta$ -T44A allele are more sensitive to pain and have increased activation of neurons in the TNC after treatment with a common migraine trigger, NTG. CKI $\delta$ -T44A mice also show a reduced threshold for CSD, increased frequency of CSD episodes, and greater arterial dilation with CSD. Astrocytes from CKI $\delta$ -T44A mice show increased spontaneous and evoked calcium signaling.

Migraine is frequent (~12% prevalence) in the general population, and it is unclear at this point what underlying genetic variants contribute to this frequency. Multiple loci that increase susceptibility to migraine have been identified (9–11, 13), and environmental factors could also play a role. In some cases, migraine is almost certainly caused by common complex genetic risk alleles segregating in the population. It is also possible that some alleles are autosomal dominant or autosomal recessive, but can be difficult to recognize as such because of polygenic genetic risk alleles segregating in the same families harbor-

ing the Mendelian alleles. This may be the case for the kindred reported here in which there are individuals with migraine who did not carry the migraine-associated CKI $\delta$  allele.

Of 11 mutation carriers, 10 were classified as affected and 1 was classified as probably affected. Comparison of the number of mutant allele carriers with migraine (10 of 11) to the noncarriers with migraine (5 of 13) using a Fisher's exact test yielded a  $P$  value of 0.011. One would not expect association of CKI $\delta$  alleles with migraine at that high frequency by chance. Nonetheless, the fact that migraine occurred in some family members who did not express a mutant CKI $\delta$  allele suggests that each family may have other predispositions to the condition.

The association between two independent mutant CKI $\delta$  alleles and the migraine phenotype suggests that these mutations contribute to the pathogenesis of migraine. Further strengthening this argument are *in vitro* and *in vivo* mouse data that support a possible causative role of these variants in migraine.

Migraine is associated with increased sensitivity to all sensory modalities, and there is growing evidence that cutaneous allodynia is a

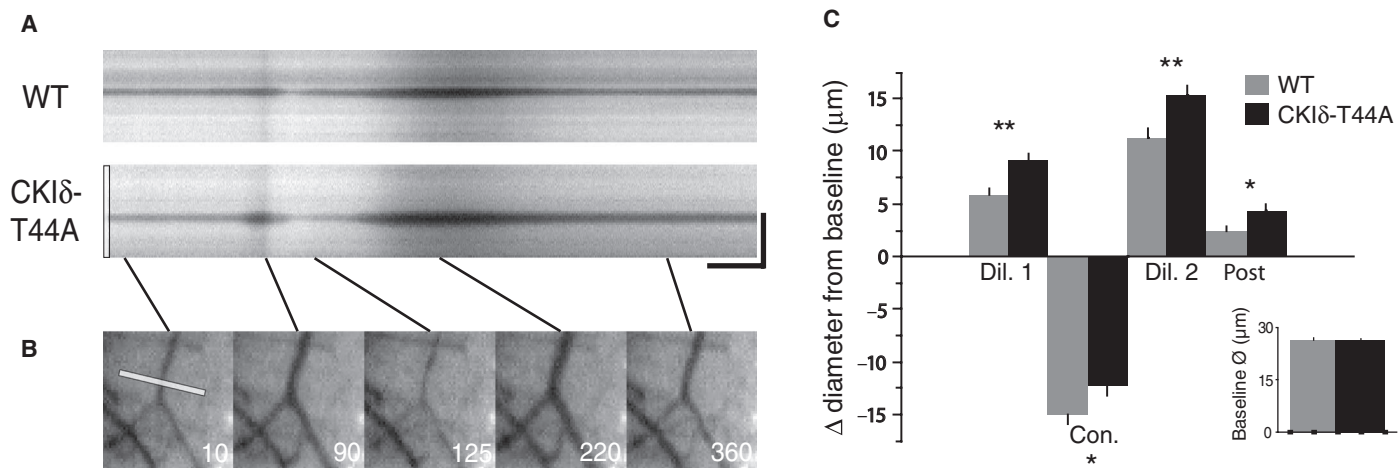


**Fig. 5. Increased dilation and decreased constriction to CSD in CKI $\delta$ -T44A mice.** (A) Arterial diameter changes in wild-type and CKI $\delta$ -T44A mice during CSD. Kymographs reveal arterial diameter changes during acute CSD. CSD is associated with arterial dilation that precedes the parenchymal CSD wavefront (Fig. 4A), followed by constriction, a second dilation, and a post-CSD dilation. Scale bar, 25 s, 125  $\mu\text{m}$ . (B) The first image shows the line drawn across the artery at baseline that generates CKI $\delta$ -T44A kymograph. The following panels show each of the CSD-associated phases of arterial activity. (C) Mean arterial diameter changes. Despite nearly identical baseline

diameters ( $26.4 \pm 0.7$  versus  $26.3 \pm 0.5 \mu\text{m}$ ;  $P = 0.94$ ) in wild-type and CKI $\delta$ -T44A mice, dilation is more prominent and constriction is less marked in CKI $\delta$ -T44A versus wild-type arteries. Initial dilation ( $32.2 \pm 0.9 \mu\text{m}$  versus  $35.6 \pm 0.7 \mu\text{m}$ ;  $P = 0.00008$ ), second dilation ( $37.7 \pm 1.3 \mu\text{m}$  versus  $41.7 \pm 1.0 \mu\text{m}$ ;  $P = 0.002$ ), and post-CSD ( $28.8 \pm 0.8 \mu\text{m}$  versus  $30.7 \pm 0.8 \mu\text{m}$ ;  $P = 0.01$ ) were all more dilated compared to baseline, and constriction was attenuated ( $11.4 \pm 1.0 \mu\text{m}$  versus  $14.1 \pm 0.9 \mu\text{m}$ ;  $P = 0.02$ , linear mixed-effects model with post hoc Tukey test) (wild type:  $n = 6$  mice, 23 vessels, 67 measurements; CKI $\delta$ -T44A:  $n = 9$  mice, 34 vessels, 110 measurements).

quantifiable marker of the disorder (33, 34). Hyperalgesia evoked by the migraine trigger NTG in mice is a model for this allodynia (19). Increased NTG-evoked mechanical and thermal hyperalgesia exhibited by CKI $\delta$ -T44A mice is consistent with a role for CKI $\delta$  in sensory hypersensitivity that is relevant to migraine. Increased NTG-induced activation of c-fos-positive nuclei in the trigeminal dorsal horn of CKI $\delta$ -T44A mice indicates increased activation of neurons associated with craniofacial pain in comparison to wild type (21, 35). CKI $\delta$ -T44A mice thus show both behavioral and functional anatomical evidence of altered craniofacial nociception.

CKI $\delta$ -T44A mice showed both a significant reduction in the threshold for evoking CSD and an increased number of CSD events elicited by continuous stimulation, consistent with increased cortical excitability that has been observed in patients with migraine. A similar susceptibility to CSD has been observed in mice expressing mutations in a P/Q-type  $\text{Ca}^{2+}$  channel and a  $\text{Na}^+/\text{K}^+$  adenosine triphosphatase that are responsible for familial hemiplegic migraine types I and II, respectively (28, 36, 37). In addition to the difference in the susceptibility to CSD, the cortical vascular response to CSD is altered in CKI $\delta$ -T44A mice. Cortical and meningeal vessels contain trigeminal afferents and transmit nociceptive signals (21, 23); the altered vascular response to CSD in CKI $\delta$ -T44A mice could be relevant to migraine-related pain.

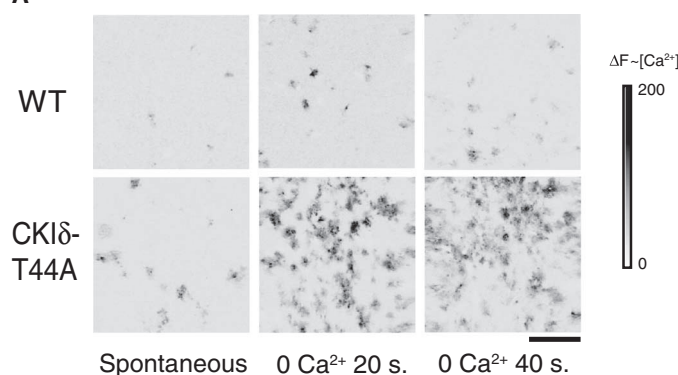
Increased spontaneous and evoked  $\text{Ca}^{2+}$  signaling in astrocytes from CKI $\delta$ -T44A mice compared to wild-type mice suggests that alteration in astrocyte signaling could be a mechanism by which the CKI $\delta$ -T44A mutation influences cortical excitability and associated vascular responses. Astrocyte  $\text{Ca}^{2+}$  waves are consistently observed in conjunction with CSD (29, 38, 39), and astrocyte signaling plays an important role in neurovascular coupling (40). Astrocytes release extracellular messengers including ATP and glutamate through undocked connexin channels

(hemichannels) (31, 41). Hypophosphorylation of connexin43 increases the proportion of connexin molecules existing as hemichannels in astrocytes compared with gap junctions, potentially leading to increased release of ATP and glutamate (30, 31, 41). We showed that connexin43 was hypophosphorylated by both mutant forms of CKI $\delta$  (Fig. 1) and that spontaneous and induced calcium signaling (Fig. 6), but not ATP release (fig. S5), was greater in cultured CKI $\delta$ -T44A astrocytes compared to wild type. Together, these findings suggest possible astrocytic mechanisms by which CKI $\delta$  mutations could predispose to migraine.

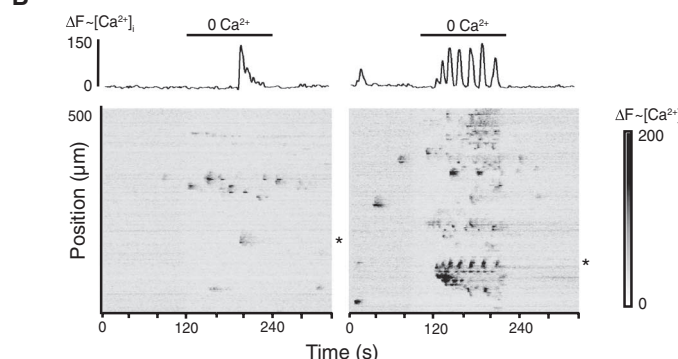
The relationship between the sleep phenotype and the migraine phenotype in individuals with alterations in the function of CKI $\delta$  is uncertain. Migraine can be modulated by sleep, and associations between migraine and a number of different sleep disorders have been reported (42). Mice expressing mutant alleles responsible for familial hemiplegic migraine type 1 have a circadian phenotype consisting of enhanced circadian phase resetting (43). Common cellular mechanisms may be involved in circadian function and episodic changes in brain excitability that cause migraine. On the other hand, migraine has not been reported as a part of the phenotype of other families with FASPS, indicating that the mechanisms underlying the migraine phenotype in families with CKI $\delta$  mutations may be distinct from those that cause alterations in sleep. Another interpretation is that CKI $\delta$  mutant families have a genetic background that enhances susceptibility to sleep phase-associated migraine triggers.

In summary, we have shown that mutations in CKI $\delta$  may contribute to the pathogenesis of human migraine and that mice expressing the CKI $\delta$ -T44A mutant enzyme show phenotypic features resembling those seen in the human disorder. The proteins encoded by all previously identified migraine genes are ion channels or pumps. CKI $\delta$ , in contrast, is an enzyme that modulates the functions of a variety of

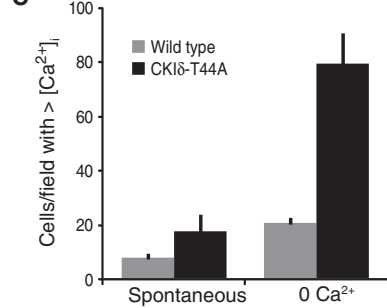
A



B



C



type mice. Scale bar, 100  $\mu$ m. (B) Raster plots show pattern of Ca<sup>2+</sup> signaling changes at baseline and upon exposure to 0 Ca<sup>2+</sup> medium in wild-type (left) and CKI $\delta$ -T44A (right) astrocyte cultures. Traces (above raster plots) show the calcium response of a representative cell (indicated by asterisks) in wild-type and CKI $\delta$ -T44A cultures. (C) Average number of cells in a 600  $\times$  600- $\mu$ m field of cultured cortical astrocytes that show an increase in intracellular Ca<sup>2+</sup> concentrations during 2 min under basal conditions (spontaneous) or during exposure to 0 Ca<sup>2+</sup> medium (evoked). Error bars represent SEM. Significantly more astrocytes from CKI $\delta$ -T44A show spontaneous ( $P = 0.0008$ ) and 0 Ca<sup>2+</sup>-evoked increases in intracellular Ca<sup>2+</sup> concentrations compared to wild-type mice ( $P = 0.0006$ ) [ $n = 16$  cultures, 200 cells per culture from eight different CKI $\delta$ -T44A mice, and 12 cultures, 200 cells per culture from six different wild-type mice (two-tailed *t* test for samples of unequal variance for each comparison)].

proteins, a subset of which could contribute to migraine pathogenesis. Identifying protein targets of CKI $\delta$  that are relevant to migraine may further elucidate the cellular signaling mechanisms underlying migraine, and identify new therapeutic approaches.

## MATERIALS AND METHODS

### Genetic association

The family members originally sought medical attention for symptoms of migraine, but during the course of evaluation, multiple individuals were also diagnosed with advanced sleep phase syndrome. Subjects signed consent or assent forms approved by the Institutional Review Boards at the University of California at San Francisco (UCSF) or the University of Utah. They then underwent physical and neurological examinations and structured interviews related to self-reported migraine traits and symptoms, circadian and sleep traits, and general health. Individuals were diagnosed with headache disorders according to the criteria of the ICHD-2. Individuals not meeting either “affected” or “unaffected” criteria were considered to be of “unknown” phenotype. Blood sample collection and DNA preparation were performed as previously described (14).

### Polymerase chain reaction and Sanger sequencing of DNA samples

CKI $\delta$  was screened for mutations via Sanger sequencing of genomic DNA. Genomic information of CKI $\delta$  coding regions was obtained from Web site databases (National Center for Biotechnology Information: <http://www.ncbi.nlm.nih.gov/> and UCSC Genome Bioinformatics: <http://genome.ucsc.edu/>) for primer design used for sequencing. Primers were designed outside of splice sites with the intent that intronic sequencing of at least 50 base pairs would flank each exon border. Twenty-five microliters of polymerase chain reactions (PCRs) was carried out per 100 ng of genomic DNA and 10 pmol of both forward and reverse primers. PCR procedures that lead to successful product amplification were as follows: 98°C, 30 s (98°C, 10 s; 60°C, 30 s; 72°C, 40 s)  $\times$  35, 72°C, 10 min, and 4°C hold. PCR product purification was done with the PCR96 Cleanup Plate (Millipore) and then sequenced. The primer set used for sequenced exon 2 of CKI $\delta$ , which harbored the T44A mutation, was as follows: forward primer, 5'-tgcttagaaggagaacacatcc-3'; reverse primer, 5'-agctgtgactgttcagg-3'.

### Protein purification and kinetic analysis

Subcloning, site-directed mutagenesis purification of enzymes, and kinase assays were performed as described (14). Briefly, reactions were conducted in 50 mM Hepes (pH 7.5), 1 mM dithiothreitol, and 1 mM MgCl<sub>2</sub> at 25°C, with catalytic amounts of CKI $\delta$ Δ317, CKI $\delta$ Δ317 T44A, or CKI $\delta$ Δ317 H46R (10 to 20 nM), 3000 Ci/mmol [ $\gamma$ -<sup>32</sup>P]ATP (1 to 500  $\mu$ M), and substrate (1 to 500  $\mu$ M, depending on the substrate,  $\alpha$ -casein or PER2 peptide). Five microliters of the reaction mixture was spotted onto P81 Whatman paper and washed with 1% phosphoric acid. Radioisotope incorporation was assayed by exposure to phosphorimage screen and quantified on a Typhoon image scanner. Saturation experimental data were fit to the Michaelis-Menten equation with KaleidaGraph (Synergy Software), and parameters  $k_{cat}$  and  $K_m$  were determined.

### Cell culture and transfection

Human embryonic kidney (HEK) 293 cells were cultured as a monolayer in Dulbecco's modified Eagle's medium (DMEM) supplemented with 10% fetal bovine serum (FBS). Cotransfection of HEK293 cells was performed with 4 mg of total DNA with Lipofectamine 2000 (Invitrogen) according to the manufacturer's protocol and as described in the figure legend. Cell treatments were carried out as described in the figure

legends. Soluble cell extracts were made in radioimmunoprecipitation assay buffer (Sigma) with PhosSTOP and Complete tabs (Roche). Protein concentration was quantified by Bradford assay (Bio-Rad).

### Immunoprecipitation and Western blotting

Immunoprecipitations were performed with anti-FLAG antibody-conjugated agarose resin (Sigma) as described by the manufacturer. Western blotting and PAGE were carried out with standard protocols.

### Animal care and handling

All protocols were approved by the Institutional Animal Care and Use Committees at UCSF and UCLA. Experiments were conducted on CKI $\delta$ -T44A line 827 (14) mice weighing between 20 and 30 g and their wild-type littermates. Animals were housed in temperature-controlled rooms on a 12-hour light-dark cycle. Experimenters were blind to the animal genotypes in all experiments.

### Nociception experiments

**NTG administration.** A stock of NTG (5 mg/ml) (American Regent Inc.) dissolved in 30% alcohol, 30% propylene glycol, and water was further diluted fresh each day in 0.9% saline in a polypropylene tube to reach desired concentrations. Doses of 1, 3, 5, 7, or 10 mg/kg were administered intraperitoneally, with a polypropylene syringe to minimize the loss of NTG activity. Control mice received an intraperitoneal injection of 0.9% saline solution without NTG.

**Behavioral assays.** Animals were habituated to each testing apparatus for 60 min on the day before and again immediately before determination of baseline nociceptive thresholds. Each set of animals underwent nociception assay before and after application of a specific dose of NTG. Behavioral assays were conducted blind to the animal genotype.

**Mechanical hypersensitivity testing.** The von Frey (Semmes-Weinstein) monofilament method was used to test mechanical sensitivity. Animals were placed on a wire mesh stand, whereas calibrated Semmes-Weinstein monofilaments (North Coast Medical) were used for the up-and-down method of determining mechanical sensation of each hind paw before injection (baseline) and 1, 2, and 4 hours after NTG injection (44). Fourteen wild-type and 15 CKI $\delta$ -T44A animals were tested. Left and right paws were scored separately for two readings per mouse per time point. Mice were given 1 hour in home cages with food and water immediately after the 2-hour measurement and were tested again 4 hours after NTG as approved by the Institutional Animal Care and Use Committees of responsible institutions.

**Thermal hypersensitivity testing.** To determine thermal hypersensitivity, the radiant heat (Hargreaves) assay focuses radiant light on the hind paw and measures the time in seconds until the mouse removes each hind paw from the source of heat (PAW Thermal Stimulator, UCSD Department of Anesthesia) (19, 45). Three determinations of response were taken for every time point with at least 2 min between each trial. The Hargreaves assay measured thermal nociceptive behaviors immediately before and 30, 60, 90, 120, and 240 min after injection of NTG. Mice were returned to home cages for 1 hour after the 2-hour measurement and were acclimated to the Hargreaves apparatus for 1 hour again before the 4-hour time point. Twenty-four CKI $\delta$ -T44A mice were tested and 22 wild-type siblings were tested for doses of 1, 3, 5, 7, and 10 mg/kg. NTG thermal sensitivity experiments were repeated with one dose (5 mg/kg) at one time point (90 min) with 12 female CKI $\delta$ -T44A and 12 wild-type siblings.

**Rotarod testing.** Nine mice of each genotype (CKI $\delta$ -T44A mice and wild-type littermates) were tested for motor function and learning on the rotarod (46). The rotating rod attained a speed of 40 rpm over a period of 5 min. Three trials separated by 1 min each were completed in each set. Each animal underwent three sets of trials for a total of nine trials. Animals were given 15-min rest between each set of the tests.

### Immunohistochemistry

CKI $\delta$ -T44A and wild-type littermates were treated with intraperitoneal injection of NTG (5 mg/kg). Two hours after NTG, mice were deeply anesthetized with isoflurane and perfused intracardially with phosphate-buffered saline (PBS) and then 4% paraformaldehyde. Whole brain and spinal cord were fixed overnight in 4% paraformaldehyde and transferred to 30% sucrose in PBS at 4°C until sectioning. Transverse 35- $\mu$ m sections of frozen spinal cord and brain were cut. Free floating sections were incubated in PBS and 0.3% Triton X-100 and 5% normal goat serum (NGS-T) for 1 hour before incubation in primary anti-Fos (Oncogene Science) at a dilution of 1:40,000 in 5% NGS-T for 18 hours at 4°C. Sections were washed in PBS before incubation for 1 hour in biotinylated goat anti-rabbit antibody (Vector Laboratories), washed in PBS, and incubated in ExtrAvidin-Peroxidase (Sigma-Aldrich Biotechnology) for 1 hour, followed by detection of the peroxidase with 3,3'-diaminobenzidine (Sigma). Mounted and coverslipped sections were counted for Fos-reactive nuclei by a single blinded observer. Fos-positive cells were counted in TNC, C1 dorsal horn, or C2 dorsal horn in 6 to 10 sections per animal ( $n = 6$  wild-type and 7 CKI $\delta$ -T44A mice). Sections were excluded if the tissue was torn or damaged. Sections were visualized with an Olympus CX41 upright light microscope. Photographs were taken with a PixeLINK PL-A662 and captured with the PixeLINK Capture software. A two-tailed Student's *t* test was used to determine statistical significance.

### CSD experiments

Anesthesia was induced (5%) and maintained (0.8 to 1.5%) with isoflurane. Temperature was maintained at  $37 \pm 0.5^\circ\text{C}$  with a rectal temperature probe and homeothermic blanket. A pulse oximetry probe was placed on the right hindpaw (8600 V, Nonin), and hemoglobin saturation was maintained at >95%. Anesthetic levels were adjusted to maintain the animal in burst suppression on field potential recordings, with an interburst interval of 4 to 9 s (47). At this anesthetic depth, the animal had no response to noxious stimulation. There were no significant differences in anesthetic level, temperature, hemoglobin saturation, or field potential burst duration or interburst interval between wild-type and CKI $\delta$ -T44A mice ( $P > 0.3$  for all comparisons, Student's *t* test).

Each animal was placed in a stereotaxic frame (Kopf Instruments), and the parietal skull was exposed. The skull was thinned to transparency, to boundaries 1 mm from temporal ridge, sagittal suture, bregma, and lambda. A glass recording electrode (~20- $\mu$ m diameter, 1 M KCl fill solution, ~0.5-megohm resistance) was advanced 550  $\mu$ m into the cortex through a burr hole placed 0.5 mm anteromedial to lambda to collect field potentials. A silver-silver chloride ground wire was placed in the neck musculature. A second burr hole was placed 0.5 mm from the temporal ridge midway between bregma and lambda for CSD induction. A 34-gauge fused silica micropipette filled with 1 M KCl and attached to a pneumatic pico-pump (MicroFil and PV-820, WPI) was carefully apposed to the cortex in the second burr hole.

The animal was placed on the imaging stage of a custom microscope and rested under anesthesia for 1 hour before imaging. The cor-

tex was illuminated with white light (5500 K, 400- to 700-nm spectral range, Philips Lumileds). Reflected light was collected for OIS with a lens system consisting of two  $f/0.95$  lenses connected front to front, focused on a high-sensitivity (0.00015 lux) 8-bit charge-coupled device camera (Wattec 902K). Field of view was  $4.2 \times 3.2$  mm, and pixel size was  $6.6 \mu\text{m}$ . Images were acquired at 2 Hz for 1 hour. Field potentials were acquired (bandpass, 0 to 1 kHz), amplified (A-M Systems 3000), digitized (at 1 kHz; PCI-6251, National Instruments), and recorded and synchronized with imaging data by a custom LabView Virtual Instrument (National Instruments).

CSD thresholding consisted of a series of pulses with progressively increasing pressure ejecting increasing volumes of KCl from the pipette (4 to 40 psi in 2-psi increments at 300-s intervals, corresponding to KCl volumes of 0.2 to  $1.4 \mu\text{l}$ ) until threshold for CSD was achieved (24). After determination of threshold, repeat inductions were performed at threshold levels every 10 min for a total of six KCl ejections. Volume ejected from the KCl pipette was verified before and after each experiment to ensure replicable thresholds. The KCl method of thresholding was used because it allowed focal administration of the KCl stimulus (electrical stimulation causes more diffuse activation and thus arterial dilation, which impedes measurement of CSD-associated vascular parameters). After thresholding, the animal was euthanized with 5% isoflurane followed by nitrogen asphyxia.

To test the rate of CSD in response to a constant stimulus, we positioned the KCl pipette just over the burr hole without touching the brain, and a 4-psi tonic output from the pneumatic pico-pump produced a constant flow of 1 M KCl into the burr hole during the course of an hour-long experiment.

Image analysis was performed with ImageJ [National Institutes of Health (NIH), Bethesda, MD] and IGOR Pro (WaveMetrics). Normalized reflectance images ( $r/r_0 \times 100$ ) were generated by dividing each frame by an average of the first 10 frames of the experiment. To generate an optical trace of CSD, we traced a 100-pixel curved line region of interest (ROI) along the CSD wavefront at the point where it contacted the field potential electrode. Each pixel of the ROI generated a trace of the CSD waveform, synchronous with electrophysiological changes, which could be compared with the other traces in each experiment as well as with separate experiments. Surface arteries were identified by morphology and by reactivity to CSD, as previously described (27). To sample vessels in an unbiased manner, we divided each imaging field into quadrants. The arterial segment closest to the center of each quadrant was chosen for analysis, yielding four arterial ROIs per experiment. A 50-pixel (330- $\mu\text{m}$ ) line ROI was placed perpendicular to the long axis of the vessel. When plotted over the course of the experiment, this line ROI revealed the diameter of the vessel, which could be computed via pixel count (Threshold and Measure Functions, ImageJ). ROIs ( $6 \times 6$  pixels) were placed immediately adjacent to the line ROIs that were used to measure arterial diameter. These allowed comparison of parenchymal and arterial changes in the same location.

OIS and field potential amplitudes and durations were measured after detecting the critical points in the respective intrinsic signal and field potential traces. This was done by computing the second derivative of each data set, allowing points of maximum change in slope to be identified. Five critical points were typically seen for intrinsic signal data: at the onset of changes, at the minimum of the first phase, at the maximum of the second phase, at the minimum of the third phase, and during a return to baseline levels (Fig. 3B). Three critical points

were found for field potential data: at the onset, maximum, and recovery of dc shift, respectively (Fig. 3B). OIS duration was calculated between the first and fourth critical points, and area under the curve was computed separately for each phase using its boundary critical points. dc shift duration was calculated between the first and third field potential critical points, and amplitude was calculated between the first and second critical points.

### Calcium imaging of astrocytic cultures

Astrocyte cultures were prepared from 1-day postnatal mouse pups (31). Cortices were removed, mechanically dissociated, and filtered as above, but the cells were resuspended and plated on glass coverslips in DMEM/F12 medium supplemented with 5% FBS. At days 4 to 7 in culture, cells were mechanically shaken for 30 min per day, and non-adherent cells were removed. Cells were cultured for 14 days before experimentation.

Changes in intracellular calcium concentration were recorded with a custom confocal microscope as previously described (48). Briefly, cells were loaded with the calcium indicator fluo4 by bath exposure to 5  $\mu\text{M}$  fluo4 acetomethoxy ester (Molecular Probes) for 30 min. Cells were washed repeatedly to remove excess indicator and then placed on the stage of a modified Nikon Diaphot microscope (Nikon Instruments). Excitation from a 475-nm diode laser was scanned via resonance mirrors to the coverslip through a  $20 \times 0.90$  numerical aperture (Olympus) objective. Fluorescence emission was collected through a 535-nm bandpass filter to a photomultiplier tube (Hamamatsu), and images were acquired at 5 Hz at a pixel resolution of  $940 \times 720$  by an image acquisition board (Raven, BitFlow) controlled by Video Savant (IO Industries) software. Solutions containing glutamate, N-methyl-D-aspartate (NMDA), or 0  $\text{Ca}^{2+}$  were applied by bath exchange.

ROIs were placed on all cells in each microscopic field, and values for fluo4 fluorescence versus time were determined for each cell in the field for each experiment. Line traces and raster plots were generated from normalized images ( $\Delta F/F_0$ ).

### ATP release

Assays of released ATP were performed with methods similar to those previously described (31). Astrocyte cultures were prepared as above and grown in plastic dishes. To measure basal ATP release, we replaced the medium above the cultures with 0.7 ml of Hanks' balanced salt solution (HBSS) for 1 min. This medium was then removed, immediately frozen, and replaced with HBSS with no added  $\text{Ca}^{2+}$  and  $\text{Mg}^{2+}$  for 1 min, after which this medium was also collected and frozen. ATP assays were performed with the Enlighten assay kit (Promega) with luminescence measurements performed with a Wallac Victor plate reader. The concentration of ATP released into normal medium in 1 min was subtracted from that released in low  $\text{Ca}^{2+}/\text{Mg}^{2+}$  medium in 1 min to determine the amount of stimulated ATP release.

### Statistical testing

Unless otherwise noted, one-way ANOVA or Student's *t* test was used, after determination that data sets were parametric. Post hoc testing was performed with Tukey test. Pearson's test was used to assess correlation between different CSD-associated measures. Statistical tests were implemented in IGOR Pro 6.0 (WaveMetrics). Unless otherwise noted, error bars denote SEM.

For nociception experiments, differences in response to mechanical and thermal stimulation were examined with a linear mixed-effects

model that accounted for both the correlation between repeated measurements taken across time on each mouse and the correlation between repeated measurements taken at each time point. The means, SEs, and differences of means reported in figures and in the text are based on the mixed model. Tests of the genotype-by-time interaction (*P* values in Fig. 2) assess the difference between CKI $\delta$ -T44A and wild type across the time spectrum. Analyses were conducted with SAS (version 9.3, SAS Institute Inc.).

## SUPPLEMENTARY MATERIALS

- [www.sciencetranslationalmedicine.org/cgi/content/full/5/183/183ra56/DC1](http://www.sciencetranslationalmedicine.org/cgi/content/full/5/183/183ra56/DC1)
- Fig. S1. Alignments for *Drosophila* Dbt and mouse (m) and human (h) CKI $\delta$  and CKI $\epsilon$  proteins.
- Fig. S2. Motor function in wild-type and CKI $\delta$ -T44A mice.
- Fig. S3. Gradient of CSD thresholds by sex and genotype.
- Fig. S4. Scatterplot of CSD dc shift duration and threshold in all animals.
- Fig. S5. Astrocyte ATP release evoked by low divalent cation solution.
- Table S1. Mechanical sensitivity thresholds.
- Table S2. Thermal responses.
- Table S3. CSD-associated measures in CKI $\delta$ -T44A mice and wild-type littermates.

## REFERENCES AND NOTES

- W. F. Stewart, C. Wood, M. L. Reed, J. Roy, R. B. Lipton; AMPP Advisory Group, Cumulative lifetime migraine incidence in women and men. *Cephalgia* **28**, 1170–1178 (2008).
- L. J. Stovner, K. Hagen, R. Jensen, Z. Katsarava, R. Lipton, A. Scher, T. Steiner, J. A. Zwart, The global burden of headache: A documentation of headache prevalence and disability worldwide. *Cephalgia* **27**, 193–210 (2007).
- M. E. Bigal, J. N. Liberman, R. B. Lipton, Age-dependent prevalence and clinical features of migraine. *Neurology* **67**, 246–251 (2006).
- M. B. Russell, J. Olesen, The genetics of migraine without aura and migraine with aura. *Cephalgia* **13**, 245–248 (1993).
- W. F. Stewart, J. Staffa, R. B. Lipton, R. Ottman, Familial risk of migraine: A population-based study. *Ann. Neurol.* **41**, 166–172 (1997).
- M. De Fusco, R. Marconi, L. Silvestri, L. Atorino, L. Rampoldi, L. Morgante, A. Ballabio, P. Aridon, G. Casari, Haploinsufficiency of ATP1A2 encoding the Na<sup>+</sup>/K<sup>+</sup> pump  $\alpha 2$  subunit associated with familial hemiplegic migraine type 2. *Nat. Genet.* **33**, 192–196 (2003).
- M. Dichgans, T. Freilinger, G. Eckstein, E. Babini, B. Lorenz-Dieperoux, S. Biskup, M. D. Ferrari, J. Herzog, A. M. van den Maagdenberg, M. Pusch, T. M. Strom, Mutation in the neuronal voltage-gated sodium channel SCN1A in familial hemiplegic migraine. *Lancet* **366**, 371–377 (2005).
- R. A. Ophoff, G. M. Terwindt, M. N. Vergouwe, R. van Eijk, P. J. Oefner, S. M. Hoffman, J. E. Lamerdin, H. W. Mohrenweiser, D. E. Bulman, M. Ferrari, J. Haan, D. Lindhout, G. J. van Ommen, M. H. Hofker, M. D. Ferrari, R. R. Frants, Familial hemiplegic migraine and episodic ataxia type-2 are caused by mutations in the Ca<sup>2+</sup> channel gene CACNL1A4. *Cell* **87**, 543–552 (1996).
- D. I. Chasman, M. Schürks, V. Anttila, B. de Vries, U. Schminke, L. J. Launer, G. M. Terwindt, A. M. van den Maagdenberg, K. Fendrich, H. Völzke, F. Ernst, L. R. Griffiths, J. E. Buring, M. Kallela, T. Freilinger, C. Kubisch, P. M. Ridker, A. Palotie, M. D. Ferrari, W. Hoffmann, R. Y. Zee, T. Kurth, Genome-wide association study reveals three susceptibility loci for common migraine in the general population. *Nat. Genet.* **43**, 695–698 (2011).
- T. Wieser, J. Pascual, A. Oterino, M. Soso, M. Barmada, K. L. Gardner, A novel locus for familial migraine on Xp22. *Headache* **50**, 955–962 (2010).
- V. Anttila, H. Stefansson, M. Kallela, U. Todt, G. M. Terwindt, M. S. Calafato, D. R. Nyholt, A. S. Dimas, T. Freilinger, B. Müller-Myhsok, V. Arto, M. Inouye, K. Alakurtti, M. A. Kaunisto, E. Härmäläinen, B. de Vries, A. H. Stam, C. M. Weller, A. Heinze, K. Heinze-Kuhn, I. Göbel, G. Borck, H. Göbel, S. Steinberg, C. Wolf, A. Björnsson, G. Gudmundsson, M. Kirchmann, A. Hauge, T. Werge, J. Schoenen, J. G. Eriksson, K. Hagen, L. Stovner, H. E. Wichmann, T. Meitinger, M. Alexander, S. Moebus, S. Schreiber, Y. S. Aulchenko, M. M. Breteler, A. G. Uitterlinden, A. Hofman, C. M. van Duijn, P. Tikka-Kleemola, S. Vepsäläinen, S. Lucae, F. Tozzi, P. Muglia, J. Barrett, J. Kaprio, M. Farkkila, L. Peltonen, K. Stefansson, J. A. Zwart, M. D. Ferrari, J. Olesen, M. Daly, M. Wessman, A. M. van den Maagdenberg, M. Dichgans, C. Kubisch, E. T. Dermizakis, R. R. Frants, A. Palotie; International Headache Genetics Consortium, Genome-wide association study of migraine implicates a common susceptibility variant on 8q22.1. *Nat. Genet.* **42**, 869–873 (2010).
- T. Freilinger, V. Anttila, B. de Vries, R. Malik, M. Kallela, G. M. Terwindt, P. Pozo-Rosich, B. Winsvold, D. R. Nyholt, W. P. van Oosterhout, V. Arto, U. Todt, E. Härmäläinen, J. Fernández-Morales, M. A. Louter, M. A. Kaunisto, J. Schoenen, O. Raitakari, T. Lehtimäki, M. Vila-Pueyo, H. Göbel, E. Wichmann, C. Sintas, A. G. Uitterlinden, A. Hofman, F. Rivadeneira, A. Heinze, E. Tronvik, C. M. van Duijn, J. Kaprio, B. Cormand, M. Wessman, R. R. Frants, T. Meitinger, B. Müller-Myhsok, J. A. Zwart, M. Färkkilä, A. Macaya, M. D. Ferrari, C. Kubisch, A. Palotie, M. Dichgans, A. M. van den Maagdenberg; International Headache Genetics Consortium, Genome-wide association analysis identifies susceptibility loci for migraine without aura. *Nat. Genet.* **44**, 777–782 (2012).
- R. G. Lafrenière, M. Z. Cader, J. F. Poulin, I. Andres-Enguix, M. Simoneau, N. Gupta, K. Boisvert, F. Lafrenière, S. McLaughlin, M. P. Dubé, M. M. Marcinkiewicz, S. Ramagopalan, O. Ansorge, B. Brais, J. Sequeiros, J. M. Pereira-Monteiro, L. R. Griffiths, S. J. Tucker, G. Ebers, G. A. Rouleau, A dominant-negative mutation in the TREK potassium channel is linked to familial migraine with aura. *Nat. Med.* **16**, 1157–1160 (2010).
- Y. Xu, Q. S. Padiath, R. E. Shapiro, C. R. Jones, S. C. Wu, N. Saigoh, K. Saigoh, L. J. Ptáček, Y. H. Fu, Functional consequences of a CKI $\delta$  mutation causing familial advanced sleep phase syndrome. *Nature* **434**, 640–644 (2005).
- U. Knippschild, A. Gocht, S. Wolff, N. Huber, J. Löbler, M. Stöter, The casein kinase 1 family: Participation in multiple cellular processes in eukaryotes. *Cell. Signal.* **17**, 675–689 (2005).
- Headache Classification Subcommittee of the International Headache Society, The International Classification of Headache Disorders: 2nd edition. *Cephalgia* **24** (Suppl. 1), 9–160 (2004).
- M. Theis, R. Jauch, L. Zhuo, D. Speidel, A. Wallraff, B. Döring, C. Frisch, G. Söhle, B. Teubner, C. Euwens, J. Huston, C. Steinhäuser, A. Messing, U. Heinemann, K. Willecke, Accelerated hippocampal spreading depression and enhanced locomotor activity in mice with astrocyte-directed inactivation of connexin43. *J. Neurosci.* **23**, 766–776 (2003).
- I. Christiansen, L. L. Thomsen, D. Daugaard, V. Ulrich, J. Olesen, Glyceryl trinitrate induces attacks of migraine without aura in sufferers of migraine with aura. *Cephalgia* **19**, 660–667 (1999).
- E. A. Bates, T. Nikai, K. C. Brennan, Y. H. Fu, A. C. Charles, A. I. Basbaum, L. J. Ptáček, A. H. Ahn, Sumatriptan alleviates nitroglycerin-induced mechanical and thermal allodynia in mice. *Cephalgia* **30**, 170–178 (2010).
- R. J. Storer, P. J. Goadsby, Trigeminovascular nociceptive transmission involves N-methyl-d-aspartate and non-N-methyl-d-aspartate glutamate receptors. *Neuroscience* **90**, 1371–1376 (1999).
- H. Bolay, U. Reuter, A. K. Dunn, Z. Huang, D. A. Boas, M. A. Moskowitz, Intrinsic brain activity triggers trigeminal meningeal afferents in a migraine model. *Nat. Med.* **8**, 136–142 (2002).
- L. Edvinsson, Tracing neural connections to pain pathways with relevance to primary headaches. *Cephalgia* **31**, 737–747 (2011).
- X. Zhang, D. Levy, R. Noseda, V. Kainz, M. Jakubowski, R. Burstein, Activation of meningeal nociceptors by cortical spreading depression: Implications for migraine with aura. *J. Neurosci.* **30**, 8807–8814 (2010).
- K. C. Brennan, M. Romero-Reyes, H. E. López Valdés, A. P. Arnold, A. C. Charles, Reduced threshold for cortical spreading depression in female mice. *Ann. Neurol.* **61**, 603–606 (2007).
- C. Ayata, H. Jin, C. Kudo, T. Dalkara, M. A. Moskowitz, Suppression of cortical spreading depression in migraine prophylaxis. *Ann. Neurol.* **59**, 652–661 (2006).
- A. A. P. Leao, Pial circulation and spreading depression of activity in the cerebral cortex. *J. Neurophysiol.* **7**, 391–396 (1944).
- K. C. Brennan, L. Beltrán-Parrazal, H. E. López-Valdés, J. Theriot, A. W. Toga, A. C. Charles, Distinct vascular conduction with cortical spreading depression. *J. Neurophysiol.* **97**, 4143–4151 (2007).
- D. Eikermann-Haerter, E. Dilekçöz, C. Kudo, S. I. Savitz, C. Waeber, M. J. Baum, M. D. Ferrari, A. M. J. M. van den Maagdenberg, M. A. Moskowitz, C. Ayata, Genetic and hormonal factors modulate spreading depression and transient hemiparesis in mouse models of familial hemiplegic migraine type 1. *J. Clin. Invest.* **119**, 99–109 (2009).
- J. Chuquet, L. Hollender, E. A. Nimchinsky, High-resolution *in vivo* imaging of the neurovascular unit during spreading depression. *J. Neurosci.* **27**, 4036–4044 (2007).
- C. D. Cooper, P. D. Lampe, Casein kinase 1 regulates connexin-43 gap junction assembly. *J. Biol. Chem.* **277**, 44962–44968 (2002).
- C. E. Stout, J. L. Costantin, C. C. Naus, A. C. Charles, Intercellular calcium signaling in astrocytes via ATP release through connexin hemichannels. *J. Biol. Chem.* **277**, 10482–10488 (2002).
- G. Arcuino, J. H. Lin, T. Takano, C. Liu, L. Jiang, Q. Gao, J. Kang, M. Nedergaard, Intercellular calcium signaling mediated by point-source burst release of ATP. *Proc. Natl. Acad. Sci. U.S.A.* **99**, 9840–9845 (2002).
- R. Burstein, B. Collins, M. Jakubowski, Defeating migraine pain with triptans: A race against the development of cutaneous allodynia. *Ann. Neurol.* **55**, 19–26 (2004).

34. R. B. Lipton, M. E. Bigal, S. Ashina, R. Burstein, S. Silberstein, M. L. Reed, D. Serrano, W. F. Stewart; American Migraine Prevalence Prevention Advisory Group, Cutaneous allodynia in the migraine population. *Ann. Neurol.* **63**, 148–158 (2008).
35. J. D. Classey, Y. E. Knight, P. J. Goadsby, The NMDA receptor antagonist MK-801 reduces Fos-like immunoreactivity within the trigeminocervical complex following superior sagittal sinus stimulation in the cat. *Brain Res.* **907**, 117–124 (2001).
36. A. M. van den Maagdenberg, D. Pietrobon, T. Pizzorusso, S. Kaja, L. A. Broos, T. Cesetti, R. C. van de Ven, A. Tottene, J. van der Kaa, J. J. Plomp, R. R. Frants, M. D. Ferrari, A *Cacna1a* knockin migraine mouse model with increased susceptibility to cortical spreading depression. *Neuron* **41**, 701–710 (2004).
37. L. Leo, L. Gherardini, V. Barone, M. De Fusco, D. Pietrobon, T. Pizzorusso, G. Casari, Increased susceptibility to cortical spreading depression in the mouse model of familial hemiplegic migraine type 2. *PLoS Genet.* **7**, e1002129 (2011).
38. T. A. Basarsky, S. N. Duffy, R. D. Andrew, B. A. MacVicar, Imaging spreading depression and associated intracellular calcium waves in brain slices. *J. Neurosci.* **18**, 7189–7199 (1998).
39. O. Peters, C. G. Schipke, Y. Hashimoto, H. Kettenmann, Different mechanisms promote astrocyte  $\text{Ca}^{2+}$  waves and spreading depression in the mouse neocortex. *J. Neurosci.* **23**, 9888–9896 (2003).
40. D. Attwell, A. M. Buchan, S. Charpak, M. Lauritzen, B. A. Macvicar, E. A. Newman, Glial and neuronal control of brain blood flow. *Nature* **468**, 232–243 (2010).
41. Z. C. Ye, M. S. Wyeth, S. Baltan-Tekkok, B. R. Ransom, Functional hemichannels in astrocytes: A novel mechanism of glutamate release. *J. Neurosci.* **23**, 3588–3596 (2003).
42. K. C. Brennan, A. Charles, Sleep and headache. *Semin. Neurol.* **29**, 406–418 (2009).
43. F. van Oosterhout, S. Michel, T. Deboer, T. Houwen, R. C. van de Ven, H. Albus, J. Westerhout, M. J. Vansteensel, M. D. Ferrari, A. M. van den Maagdenberg, J. H. Meijer, Enhanced circadian phase resetting in R192Q  $\text{Ca}_v2.1$  calcium channel migraine mice. *Ann. Neurol.* **64**, 315–324 (2008).
44. S. R. Chaplan, F. W. Bach, J. W. Pogrel, J. M. Chung, T. L. Yaksh, Quantitative assessment of tactile allodynia in the rat paw. *J. Neurosci. Methods* **53**, 55–63 (1994).
45. K. Hargreaves, R. Dubner, F. Brown, C. Flores, J. Joris, A new and sensitive method for measuring thermal nociception in cutaneous hyperalgesia. *Pain* **32**, 77–88 (1988).
46. N. W. Dunham, T. S. Miya, A note on a simple apparatus for detecting neurological deficit in rats and mice. *J. Am. Pharm. Assoc. Am. Pharm. Assoc.* **46**, 208–209 (1957).
47. J. C. Chang, L. L. Shook, J. Biag, E. N. Nguyen, A. W. Toga, A. C. Charles, K. C. Brennan, Biphasic direct current shift, haemoglobin desaturation and neurovascular uncoupling in cortical spreading depression. *Brain* **133**, 996–1012 (2010).
48. L. Beltran-Parrazal, H. E. López-Valdés, K. C. Brennan, M. Díaz-Muñoz, J. de Vellis, A. C. Charles, Mitochondrial transport in processes of cortical neurons is independent of intracellular calcium. *Am. J. Physiol. Cell Physiol.* **291**, C1193–C1197 (2006).

**Acknowledgments:** We thank A. Ring for helpful discussion, E. Quinn and W. Waheed for assistance with clinical data acquisition, N. Blades for statistical expertise, and the families who participated in these studies. **Funding:** This work was supported by NIH K08-NS059072 and R21-NS070084 and the American Headache Society (to K.C.B.), the A.P. Giannini Foundation (to E.A.B.), Department of Defense PR10085 and The Migraine Research Foundation (to A.C.C.), NIH R01-GM079180 (to Y.-H.F.), and NIH R01-HL59596 and the Sandler Neurogenetic Fund (to Y.-H.F. and L.J.P.). L.J.P. is an Investigator of the Howard Hughes Medical Institute (HHMI). **Author contributions:** R.E.S., A.C.C., and L.J.P. conceived the study; K.C.B., E.A.B., W.C.H., and A.C.C. designed the experiments; K.C.B., E.A.B., R.E.S., J.Z., W.C.H., Y.H., H.-Y.L., C.R.J., Y.-H.F., and A.C.C. performed the experiments or collected the data; K.C.B., E.A.B., R.E.S., W.C.H., and A.C.C. analyzed the data; K.C.B., E.A.B., R.E.S., A.C.C., and L.J.P. wrote the paper. **Competing interests:** The authors declare that they have no competing interests. **Data and materials availability:** All published reagents will be shared according to NIH and HHMI guidelines.

Submitted 24 January 2013

Accepted 7 March 2013

Published 1 May 2013

10.1126/scitranslmed.3005784

**Citation:** K. C. Brennan, E. A. Bates, R. E. Shapiro, J. Zyuzin, W. C. Hallows, Y. Huang, H.-Y. Lee, C. R. Jones, Y.-H. Fu, A. C. Charles, L. J. Ptáček, Casein kinase I $\delta$  mutations in familial migraine and advanced sleep phase. *Sci. Transl. Med.* **5**, 183ra56 (2013).

# Migraine: a brain state

Andrew Charles

## Purpose of review

Migraine has traditionally been categorized as a pain disorder, focusing on headache as its central feature. This narrow view does not account for the complex array of premonitory and postdromal symptoms that occur in the hours before and after headache. This review outlines evidence that supports a broader view of migraine as a pathological brain state.

## Recent findings

Studies of the clinical features of a migraine attack, in combination with imaging and electrophysiological studies, provide evidence that migraine involves widespread changes in brain function and connectivity. These changes parallel those seen in other brain states such as sleep. Neurochemical mediators, including adenosine, and nonsynaptic signalling mechanisms involving astrocytes may play a role in the migraine state.

## Summary

Consideration of a migraine attack as a brain state provides an expanded framework for understanding all of its symptoms, and the underlying alterations in the activity of multiple brain networks. Mechanisms driving the transition to the migraine state may represent novel targets for acute and preventive therapies.

## Keywords

adenosine, astrocytes, headache, resting states, sleep

## INTRODUCTION

Brain states such as sleep, wakefulness and attention are characterized by consistent patterns of brain activity, the coordinated involvement of multiple brain regions or networks, and stereotyped associated behaviours or functional responses [1,2]. A migraine attack clearly includes all of these features, and therefore can be practically considered as a pathological brain state. What is the purpose of defining migraine in this way? Traditional definitions have naturally focused on headache, the most prominent symptom of migraine. But consideration of migraine simply as a 'trigemino-vascular' disorder or a pain disorder does not account for the complex constellation of migraine symptoms that precede, accompany or outlast headache. A more comprehensive definition of a migraine attack provides a context for a more definitive understanding of the disorder and for the development of novel and effective therapies. This review will summarize recent studies that support the concept of migraine as a brain state.

## CLINICAL FEATURES OF THE MIGRAINE STATE

There are several parallels between the migraine state and the sleep state. Similar to sleep, there are

homeostatic, circadian and allostatic factors [3,4<sup>\*</sup>] that drive the initiation of a migraine attack. Food intake, fatigue, time of day, hormonal changes and stress are among the many variables that may be involved in the onset of migraine, just as they are with sleep. Also similar to the sleep state, multiple brain networks are either activated or inactivated during a migraine attack. Most studies of brain networks in migraine have focused on those involved in the perception and processing of pain [5<sup>\*\*</sup>,6<sup>\*\*\*</sup>,7<sup>\*\*\*\*</sup>]. As discussed below, however, the clinical symptoms of migraine as well as electrophysiological and functional imaging studies indicate involvement of multiple brain networks in addition to those directly related to pain. One possibility is that migraine involves a disruption of the normal coordination between different brain networks that occurs during physiological brain states. With sleep, there

Headache Research and Treatment Program, Department of Neurology, David Geffen School of Medicine at UCLA, Los Angeles, California, USA

Correspondence to Andrew Charles, MD, Headache Research and Treatment Program, Department of Neurology, David Geffen School of Medicine at UCLA, Los Angeles, CA 90095, USA. Tel: +1 310 794 1870; fax: +1 310 206 6906; e-mail: acharles@ucla.edu

*Curr Opin Neurol* 2013, 26:235–239

DOI:10.1097/WCO.0b013e32836085f4

**KEY POINTS**

- The diverse clinical features and widespread patterns of brain activity associated with a migraine attack are consistent with a pathological brain state.
- The migraine state may involve derangements of mechanisms involved in the maintenance of and switching between physiological brain states.
- Neurochemical mediators such as adenosine and nonsynaptic mechanisms involving astrocytes similar to those that initiate sleep may also play a role in the migraine state.

is coordinated activation of sleep-promoting networks and inhibition of wake-promoting networks [3]. Similarly, in most normal physiological states (with the exception of rapid eye movement sleep), arousal is coordinated with awareness [8]. By contrast, in some pathological states such as the vegetative state and sleepwalking, there may be relatively greater arousal than awareness. The migraine state represents the opposite situation, wherein decreased arousal (as indicated by the symptoms of yawning, fatigue and somnolence) is accompanied by heightened awareness (as indicated by increased sensitivity to light, sound, smell and touch). This clinical picture suggests that in addition to activation of pain networks, the migraine state involves a derangement of the normal physiological relationship between other brain networks such as those regulating sleep, wakefulness, awareness and arousal.

Hypotheses of migraine pathogenesis have typically focused on a primary region of initiation such as spreading depression in the cortex or a 'migraine generator' in the brainstem. But the temporal progression of a migraine attack indicates simultaneous changes in the function of multiple brain regions, and it is not clear that there is a single anatomical region wherein migraine begins in all patients. Premonitory symptoms occurring up to hours before headache, including neck pain, fatigue, mood change, yawning, polyuria and light sensitivity, may last into the headache phase of an attack and extend into the postdrome lasting hours following resolution of headache [9–12]. Similarly, prospective recording of symptoms indicates that headache, light sensitivity and nausea commonly occur at the same time as aura [13<sup>\*</sup>]. Symptoms that persist after resolution of the headache include neck pain, mood change, fatigue and asthenia [11,14,15]. This overlapping pattern of symptoms is consistent with parallel alteration in the activity of different anatomical regions rather than a linear cascade of changes with one leading to the next.

**IMAGING STUDIES INDICATE WIDESPREAD CHANGES IN BRAIN FUNCTION DURING MIGRAINE**

The initial functional imaging studies of migraine highlighted changes in the activity of brainstem and cortex during a migraine attack [16–18]. More recent studies have also shown concomitant changes in the activity of other brain regions. Activation of the hypothalamus has been shown to occur during migraine [19], and this change in hypothalamic activity may be particularly important in the premonitory phase of migraine that precedes headache [20]. Such alteration of hypothalamic function could explain a number of common migraine symptoms including changes in appetite, mood and wakefulness that occur before a headache begins. Functional MRI (fMRI) studies have also recently demonstrated changes in thalamic activation during a migraine attack that are correlated with allodynia [21]. Thalamic activation could play an important role in the sensitization to all sensory modalities that occurs during a migraine attack. Previous PET and MRI studies showed dramatic changes in the activity of the occipital cortex associated with migraine visual aura [17,18], but more recent studies have also demonstrated increased activation of the occipital cortex in response to visual stimuli during a migraine attack correlated with photophobia in patients without visual aura [22<sup>\*\*</sup>]. Interestingly, this increased occipital cortical sensitivity persisted after relief of headache. Light sensitivity also commonly precedes headache in a migraine attack [12], suggesting that increased excitability of the visual system is a feature of the migraine state that can both precede and outlast headache.

fMRI techniques have been used extensively in recent studies to identify brain network activity that is characteristic of specific brain states [1,2]. This fMRI approach relies on the identification of brain regions that display correlated low frequency (<0.1 Hz) oscillations in blood oxygen level dependent signal, indicative of functional connectivity between these regions. 'Resting states' are defined as those that occur in the absence of external stimulation. The most commonly studied resting state network is the default mode network – brain regions that are more active under conditions of rest and less active during cognitive activation, including the posterior cingulate cortex, anterior cingulate cortex and medial prefrontal cortex among others [1,2,7<sup>\*\*</sup>]. It is likely that the migraine state will show characteristic changes in resting state activity, although no studies to date have reported such changes during a migraine attack. Structural and fMRI studies have demonstrated interictal alterations in connectivity

in individuals with migraine, particularly in brain networks involved in pain processing [5<sup>•</sup>,7<sup>•</sup>,23,24, 25<sup>•</sup>,26]. Interictal changes in the activity of networks involved in executive function [27<sup>•</sup>] and visual motion processing [23,28] have also been shown in migraine patients. These changes in connectivity are typically believed to be a consequence of migraine, as they are correlated with migraine frequency and duration. It is also possible, however, that these interictal structural and functional alterations contribute to disruptions in normal brain connectivity that occur *during* the migraine state.

## ELECTROPHYSIOLOGICAL FEATURES OF THE MIGRAINE STATE

Brain states may be characterized by specific patterns of electrophysiological activity as measured by electroencephalography, magnetoencephalography or evoked potentials. Although much less pronounced than those observed in other brain states, electrophysiological changes indicating extensive changes in brain activity do occur before and during a migraine attack. Quantitative electroencephalogram (EEG) studies have been reported to show increased slowing in the theta range and increased asymmetry of EEG signal in the hours preceding a migraine attack and during the attack [29<sup>•</sup>]. Evoked potential studies also show characteristic changes in activity with migraine. Somatosensory evoked potentials have a high frequency component that is believed to reflect activity in a thalamo-cortical circuit. These high frequency oscillations (HFOs) are reduced in amplitude and area between attacks, and are normalized during attacks [30]. Recent studies have found that changes in HFOs are correlated with clinical fluctuations in migraine [31<sup>•</sup>], and that HFOs can be normalized by repetitive transcranial magnetic stimulation (rTMS) [32<sup>•</sup>]. These observations suggest that changes in the activity of brain-stem arousal networks and related thalamocortical networks are involved in the initiation of migraine and provide further support for the concept of a migraine attack as a brain state.

## NEUROCHEMICAL MEDIATORS OF THE MIGRAINE STATE

A number of neurochemical mediators have been implicated in the transition from the wake to the sleep state. The transition to the migraine state may similarly involve changes in the levels of a variety of neurochemical mediators. Parallels between premonitory symptoms in migraine and those evoked by administration of dopamine receptor agonists have led to the hypothesis that dopamine may be one of

these mediators [33]. Orexins have also been proposed as potential mediators of both migraine and sleep [34]. Other interesting candidates for mediators of the migraine state that have been studied extensively in the context of sleep are the purines (ATP and adenosine) [35–37]. Extracellular adenosine levels increase during wakefulness, and a longstanding hypothesis has been that this increased adenosine plays a role in sleep induction by activation of receptors that inhibit neuronal activity [37]. An appealing aspect of this hypothesis is that it links cellular energy metabolism (adenosine is a product of ATP breakdown) and the drive to sleep, thus representing a homeostatic mechanism that may act in parallel with the hypothalamic circadian clock. ATP levels have been reported to rise during early stages of sleep in animals, supporting the hypothesis that one function of sleep is to restore a balance between ATP and adenosine [38]. Interictal magnetic resonance spectroscopy studies show a decrease in brain phosphocreatine content, and a decrease in occipital lobe ATP interictally in some migraine patients [39<sup>•</sup>], consistent with an alteration in ATP and other high energy substrates in migraine. Although there is no direct evidence for a role for adenosine in migraine, the migraine therapeutic effects of caffeine, a nonselective adenosine receptor antagonist, provide support for such a role. It is also interesting to speculate that adenosine could play a role in the fatigue, yawning and asthenia associated with migraine. The development of selective adenosine receptor antagonists for other indications may provide an opportunity for more definitive investigation of a hypothesized role for adenosine in the migraine state.

## A ROLE FOR ASTROCYTES?

Diffuse changes in the activity of multiple brain regions suggest that the migraine state may not only involve traditional neuronal circuits but also non-synaptic mechanisms that include glial cells. There is growing evidence that astrocytes play a significant role in the homeostatic mechanisms regulating the sleep/wake states, and it is reasonable to hypothesize that they may also play a role in the migraine state. Animal studies indicate that a significant proportion of the adenosine that accumulates during wakefulness may be derived from astrocytes, and this astrocyte-derived adenosine can alter synaptic function by activation of A1 receptors [40<sup>••</sup>]. Recent in-vivo studies in mice also indicate that multiple general anaesthetics selectively inhibit calcium signalling in astrocytes, raising the possibility that suppression of astrocyte activity is a mechanism of general anaesthesia [41<sup>•</sup>]. Genes expressed primarily in astrocytes

have also been implicated in migraine with and without aura, as well as in familial hemiplegic migraine, lending support to the concept that astrocytes may contribute to the diffuse changes in brain function that occur during a migraine attack [42,43]. Astrocytes show propagated waves of activity whose temporal and spatial characteristics are remarkably similar to those of cortical spreading depression, and we have suggested that these waves could be involved in propagated changes in brain activity and vascular function that are observed in patients with migraine [44]. Astrocytes are known to mediate bidirectional signalling between neurons and the vasculature, and astrocyte regulation of vascular function may be influenced by metabolic factors including adenosine levels [45]. Astrocytes could therefore play a significant role in the vascular changes and neurovascular uncoupling [46] that are observed as a part of the migraine state.

## CONCLUSION

Conceptualizing a migraine attack as a brain state facilitates consideration of the entire array of migraine symptoms, as well as its complex neurochemical, cellular and anatomical substrates. Expanding the definitions of migraine beyond the traditional narrow focus on aura and headache creates opportunities for new experimental paradigms to study the disorder, and new therapeutic approaches. Comparison of the similarities and differences between migraine and other brain states, enabled by advances in imaging and physiological recording techniques, is likely to provide critical new insight into the causes of migraine and how to more effectively treat it.

## Acknowledgements

The author is supported by the United States Department of Defense PR10085.

## Conflicts of interest

*There are no conflicts of interest.*

## REFERENCES AND RECOMMENDED

### READING

Papers of particular interest, published within the annual period of review, have been highlighted as:

- of special interest
- of outstanding interest

Additional references related to this topic can also be found in the Current World Literature section in this issue (pp. 324–325).

1. Heine L, Soddu A, Gomez F, et al. Resting state networks and consciousness: alterations of multiple resting state network connectivity in physiological, pharmacological, and pathological consciousness states. *Front Psychol* 2012; 3:295.
2. Tang YY, Rothbart MK, Posner MI. Neural correlates of establishing, maintaining, and switching brain states. *Trends Cogn Sci* 2012; 16:330–337.

3. Saper CB, Fuller PM, Pedersen NP, et al. Sleep state switching. *Neuron* 2010; 68:1023–1042.

4. Borsook D, Maleki N, Becerra L, et al. Understanding migraine through the lens of maladaptive stress responses: a model disease of allostatic load. *Neuron* 2012; 73:219–234.

This review proposes a model for the progression of migraine based on structural and functional brain changes that occur in response to stress.

5. Mainero C, Boshyan J, Hadjikhani N. Altered functional magnetic resonance imaging resting-state connectivity in periaqueductal gray networks in migraine. *Ann Neurol* 2011; 70:838–845.

Using resting state fMRI approaches, this study shows altered connectivity between the periaqueductal gray and other brain regions involved in pain processing in patients with migraine with different clinical features. These results build on previous functional imaging studies that implicate the periaqueductal gray region in migraine. The authors conclude that the results are consistent with impairment of descending antinociceptive pain pathways.

6. Russo A, Tessitore A, Esposito F, et al. Pain processing in patients with migraine: an event-related fMRI study during trigeminal nociceptive stimulation. *J Neurol* 2012; 259:1903–1912.

This study found increased activation of a specific region in the pons in response to noxious heat stimulation in migraineurs vs. controls. The authors conclude that this represents increased antinociceptive activity in migraine patients, a somewhat different conclusion than presented by Mainero *et al.* above.

7. Xue T, Yuan K, Zhao L, et al. Intrinsic brain network abnormalities in migraine without aura revealed in resting-state fMRI. *PLoS One* 2012; 7:e52927.

Altered connectivity in multiple brain networks is shown interictally in migraine patients vs. controls. The authors suggest that this indicates that migraine has deleterious effects resulting in the development of dysfunctional brain connectivity over time.

8. Cavanna AE, Shah S, Eddy CM, et al. Consciousness: a neurological perspective. *Behav Neurol* 2011; 24:107–116.

9. Giffin NJ, Ruggiero L, Lipton RB, et al. Premonitory symptoms in migraine: an electronic diary study. *Neurology* 2003; 60:935–940.

10. Kelman L. The premonitory symptoms (prodrome): a tertiary care study of 893 migraineurs. *Headache* 2004; 44:865–872.

11. Quintela E, Castillo J, Munoz P, et al. Premonitory and resolution symptoms in migraine: a prospective study in 100 unselected patients. *Cephalgia* 2006; 26:1051–1060.

12. Schoonman GG, Evers DJ, Terwindt GM, et al. The prevalence of premonitory symptoms in migraine: a questionnaire study in 461 patients. *Cephalgia* 2006; 26:1209–1213.

13. Hansen JM, Lipton RB, Dodick DW, et al. Migraine headache is present in the aura phase: a prospective study. *Neurology* 2012; 79:2044–2049.

This describes a large study in which patients prospectively recorded migraine symptoms in relation to onset of aura. It concludes that a majority of patients experienced headache and photophobia at the same time as aura, challenging the concept that aura represents a discrete phase of a migraine attack that consistently precedes the headache phase.

14. Kelman L. The postdrome of the acute migraine attack. *Cephalgia* 2006; 26:214–220.

15. Ng-Mak DS, Fitzgerald KA, Norquist JM, et al. Key concepts of migraine postdrome: a qualitative study to develop a postmigraine questionnaire. *Headache* 2011; 51:105–117.

16. Weiller C, May A, Limroth V, et al. Brain stem activation in spontaneous human migraine attacks. *Nat Med* 1998; 1:658–660.

17. Woods RP, Iacoboni M, Mazzuotta JC. Bilateral spreading cerebral hypoperfusion during spontaneous migraine headache. *N Engl J Med* 1994; 331:1689–1692.

18. Cao Y, Welch KM, Aurora S, et al. Functional MRI-BOLD of visually triggered headache in patients with migraine. *Arch Neurol* 1999; 56:548–554.

19. Denelle M, Fabre N, Payoux P, et al. Hypothalamic activation in spontaneous migraine attacks. *Headache* 2007; 47:1418–1426.

20. Sprenger T, Maniyar FH, Monteith TS, et al. Midbrain activation in the premonitory phase of migraine: a  $H_2^{15}O$ -positron emission tomography study [abstract]. *Headache* 2012; 52:863–864.

21. Burstein R, Jakubowski M, Garcia-Nicas E, et al. Thalamic sensitization transforms localized pain into widespread allodynia. *Ann Neurol* 2010; 68:81–91.

22. Denelle M, Bouloche N, Payoux P, et al. A PET study of photophobia during spontaneous migraine attacks. *Neurology* 2011; 76:213–218.

This study reports increased activation of the occipital cortex in response to light correlated with photophobia during migraine attacks. Interestingly, this increased cortical activity persisted after relief of headache, indicating a dissociation between mechanisms mediating migraine pain and those mediating sensory sensitivity.

23. Liu J, Zhao L, Li G, et al. Hierarchical alteration of brain structural and functional networks in female migraine sufferers. *PLoS One* 2012; 7:e51250.

24. DaSilva AF, Granziera C, Tuch DS, et al. Interictal alterations of the trigeminal somatosensory pathway and periaqueductal gray matter in migraine. *NeuroReport* 2007; 18:301–305.

25. Maleki N, Becerra L, Nutile L, et al. Migraine attacks the basal ganglia. *Mol Pain* 2011; 7:71.

This study found reduced activation but increased volume in the basal ganglia in patients with frequent migraine as compared with infrequent migraine. The results suggest that the basal ganglia is another brain region that contributes to migraine, consistent with the concept that migraine involves widespread changes in brain activity.

- 26.** Moulton EA, Burstein R, Tully S, et al. Interictal dysfunction of a brainstem descending modulatory center in migraine patients. *PLoS One* 2008; 3:e3799.
- 27.** Russo A, Tessitore A, Giordano A, et al. Executive resting-state network ■ connectivity in migraine without aura. *Cephalgia* 2012; 32:1041–1048.
- This study reports reduced functional connectivity of frontoparietal networks involved in executive function in patients with migraine interictally, with greater reductions in connectivity observed in patients who reported more severe attacks. Although migraine patients did not have any measurable changes in executive function based on neuropsychological testing, the results suggest that migraine is associated with subclinical changes in the connectivity of frontoparietal networks.
- 28.** Granziera C, DaSilva AF, Snyder J, et al. Anatomical alterations of the visual motion processing network in migraine with and without aura. *PLoS Med* 2006; 3:e402.
- 29.** Bjork M, Stovner LJ, Hagen K, et al. What initiates a migraine attack? ■ Conclusions from four longitudinal studies of quantitative EEG and steady-state visual-evoked potentials in migraineurs. *Acta Neurol Scand Suppl* 2011; 191:56–63.
- This is a summary of multiple quantitative EEG and evoked potential studies showing slowing and asymmetry of EEG signal, as well as reduced photic responses, in the hours preceding a migraine headache. These findings are consistent with a role for diffuse changes in thalamocortical function in the initiation of the migraine state.
- 30.** Coppola G, Vandenheede M, Di Clemente L, et al. Somatosensory evoked high-frequency oscillations reflecting thalamo-cortical activity are decreased in migraine patients between attacks. *Brain* 2005; 128:98–103.
- 31.** Restuccia D, Vollono C, Del Piero I, et al. Somatosensory high frequency oscillations reflect clinical fluctuations in migraine. *Clin Neurophys* 2012; 123:2050–2056.
- This study shows that changes in electrophysiological measures of brainstem arousal centres and thalamo-cortical activity are correlated with worsening or improvement in migraine frequency.
- 32.** Coppola G, De Pasqua V, Pierelli F, et al. Effects of repetitive transcranial ■ magnetic stimulation on somatosensory evoked potentials and high frequency oscillations in migraine. *Cephalgia* 2012; 32:700–709.
- This study demonstrates that electrophysiological abnormalities consistent with dysfunction of thalamo-cortical circuits in migraine patients can be normalized by rTMS, raising the possibility that rTMS could represent a therapeutic approach to modulating the migraine state.
- 33.** Akerman S, Goadsby PJ. Dopamine and migraine: biology and clinical implications. *Cephalgia* 2007; 27:1308–1314.
- 34.** Holland P, Goadsby PJ. The hypothalamic orexinergic system: pain and primary headaches. *Headache* 2007; 47:951–962.
- 35.** Brown RE, Basheer R, McKenna JT, et al. Control of sleep and wakefulness. *Physiol Rev* 2012; 92:1087–1187.
- 36.** Burnstock G. Introduction to purinergic signalling in the brain. *Adv Exp Med Biol* 2013; 986:1–12.
- 37.** Porkka-Heiskanen T, Kalinchuk AV. Adenosine, energy metabolism and sleep homeostasis. *Sleep Med Rev* 2011; 15:123–135.
- 38.** Dworak M, McCarley RW, Kim T, et al. Sleep and brain energy levels: ATP changes during sleep. *J Neurosci* 2010; 30:9007–9016.
- 39.** Reyngoudt H, Paemeleire K, Descamps B, et al. 31P-MRS demonstrates a ■ reduction in high-energy phosphates in the occipital lobe of migraine without aura patients. *Cephalgia* 2011; 31:1243–1253.
- This study reports reduced levels of ATP in occipital cortex of some migraine patients and confirms previous reports of reduced phosphocreatine levels in migraine patients interictally. These findings identify cortical metabolic alterations that may predispose to the migraine state and provide a rationale for migraine therapies that target brain metabolism.
- 40.** Schmitt LJ, Sims RE, Dale N, et al. Wakefulness affects synaptic and network ■ activity by increasing extracellular astrocyte-derived adenosine. *J Neurosci* 2012; 32:4417–4425.
- This study provides evidence that astrocytes are key players in homeostatic mechanisms of sleep and wakefulness through their contribution to extracellular adenosine.
- 41.** Thrane AS, Thrane VR, Zeppenfeld D, et al. General anaesthesia selectively ■ disrupts astrocyte calcium signaling in the awake mouse cortex. *Proc Natl Acad Sci U S A* 2012; 109:18974–18979.
- This study finds that spontaneous astrocyte calcium signalling, including propagated calcium responses in astrocyte networks, are suppressed by general anaesthetic agents. In addition to implicating astrocytes in the state of general anaesthesia, these results emphasize that experimental conditions involving anaesthetics are an important factor in the interpretation of studies of cellular signalling *in vivo*.
- 42.** Anttila V, Stefansson H, Kallela M, et al. Genome-wide association study of migraine implicates a common susceptibility variant on 8q22.1. *Nat Genet* 2010; 10:869–873.
- 43.** Freilinger T, Anttila V, de Vries B, et al. Genome-wide association analysis ■ identifies susceptibility loci for migraine without aura. *Nat Genet* 2012; 44:777–782.
- This large population study identifies multiple susceptibility loci for migraine without aura involving genes primarily expressed in different neural cell types and involving diverse potential functions. This, along with other recent genetic studies, indicates a wide range of potential cellular and neurochemical mechanisms that may predispose to migraine.
- 44.** Charles A, Brennan KC. Cortical spreading depression: new insights and persistent questions. *Cephalgia* 2009; 29:1115–1124.
- 45.** Gordon GR, Choi HB, Rungta RL, et al. Brain metabolism dictates the polarity of astrocyte control over arterioles. *Nature* 2008; 456:745–749.
- 46.** Wolf ME, Held VE, Forster A, et al. Pearls & oy-sters: dynamics of altered cerebral perfusion and neurovascular coupling in migraine aura. *Neurology* 2011; 77:127–128.